base] represent the sum of the concentrations for all possible species), were determined. This equilibrium differs from that of eq 10 because of the fact that it occurs in water rather than in deuterium oxide medium.

The Schiff base formation constants determined for the system PLP and APP over the pH range 7–10.5 are presented in Figure 8. Increasing concentrations of APP relative to a fixed concentration of PLP results in the formation of increasing amounts of imine, as evidenced by the increase of absorption at 274 nm. The value for K_c' is obtained by measuring the changes in absorbance (ΔA at 274 nm) with increments of amino acid concentrations and by plotting $1/\Delta A$ against $1/[\text{APP}]$ (eq 17). The intercept

$$\epsilon l K_c'[\text{PLP}]\frac{1}{\Delta A} - K_c' = \frac{1}{[\text{APP}]_T} \qquad (17)$$

of the perfectly linear plot so obtained with the abcissa[5,42,43] gave the value of K_c', where ϵ is the molar absorptivity of SB, l is the length of the cell, and K_c' is the constant for a specific pH and temperature. ΔA is the difference of the absorbance of SB and PLP. The values of K_c' are plotted in Figure 8.

The K_c' values in H_2O are in general agreement with the K_c values of the same compounds in D_2O solvent, determined by NMR. The difference observed is due to the difference in solvent. The best conditions for Schiff base formation are pH 8.8 and pD 9.7 in H_2O and D_2O, respectively. Under these conditions the difference between log K_c' and log K_c in H_2O and D_2O is 0.30. It is also seen that the protonation constants in H_2O and D_2O differ by a nearly constant amount, with the values in D_2O being roughly $0.41 + 0.020pK(H_2O)$ values higher than those obtained with H_2O as solvent.

The conditional equilibrium constants governing the degree of formation of individual Schiff base species as a function of pH or pD are not necessarily equivalent, and the small differences in the values listed are therefore reasonable.

The UV–vis measurements of formation constants in H_2O make possible comparisons of Schiff base stabilities with those of other PLP–amino phosphonic systems[5] such as aminomethylphosphonic acid and (2-aminoethyl)phosphonic acid. Of the three aminophosphonic acids studied, 2-amino-3-phosphonopropionic acid (APP) shows the lowest tendency to form Schiff bases. This lower affinity could be due principally to steric hindrance and charge repulsion between one of the negative groups of the APP residue in the Schiff base and the phosphate ester group of PLP. This interpretation seems to be supported by the use of space-filling molecular models. Coordination of the azomethine hydrogen in the APP Schiff base may occur by hydrogen bonding to either the carboxylate or phosphonate group, as indicated by formulas **8** and **9**. Because of lack of free rotation about the azomethine double bond, there will be one free negatively charged center on the Schiff base close to the monophosphonate ester at the 5′ position. Such interaction involves unfavorable charge repulsion, thus decreasing the tendency to form the Schiff base. As pointed out above, further protonation of the Schiff base at one of these positions provides an additional degree of stability (or mitigated destabilizing Coulombic repulsions) through hydrogen bonding and charge reduction.

Acknowledgment. This work was supported by a research grant, AM-11694, from the National Institute of Arthritis, Metabolic and Digestive Diseases, U.S. Public Health Service. B.S. thanks UFSC (Brazil) for fellowship support.

Registry No. 1, 54-47-7; **2**, 91239-59-7; APP, 5652-28-8; APP-PLP Schiff base, 91239-60-0.

(42) Lucas, N.; King, N. L.; Brown, S. J. *Biochem. J.* **1962**, *84*, 118.
(43) Dixon, M. *Biochem. J.* **1953**, *55*, 170.

Organosilicon Rotanes

Corey W. Carlson, Kenneth J. Haller, Xing-Hua Zhang, and Robert West*

Contribution from the Department of Chemistry, University of Wisconsin, Madison, Wisconsin 53706. *Received November 2, 1983*

Abstract: Reaction of $(CH_2)_4SiCl_2$ with 2 equiv of lithium leads to the spirocyclic organosilanes, $[(CH_2)_4Si]_n$, of which n = 5–12 have been isolated and characterized. With excess Li or K, the novel rearrangement product **3a** is formed. Reaction of $(CH_2)_5SiCl_2$ with K produces rotanes $[(CH_2)_5Si]_n$, n = 4–6. Photolysis of $[(CH_2)_4Si]_6$ or $[(CH_2)_5Si]_5$ (**5**) leads to loss of a cyclic silylene and formation of the next smaller ring. Structures of $[(CH_2)_4Si]_5$ (**1**) and of **5** were studied by single-crystal X-ray diffraction; both crystallize in space group $P2_1/c$. The silacyclohexane rings in **5** are all in the chair conformation, while the silacyclopentane rings in crystalline **1** adopt a variety of conformations.

Although the best known alkylcyclopolysilanes are the permethyl compounds, $(Me_2Si)_n$,[1-3] cyclic polysilanes containing Et, *n*-Pr, *n*-Bu, *i*-Pr, and *i*-Bu as substituents have recently been prepared.[4-6] These cyclosilanes show unusual properties which arise from electron delocalization in the Si–Si σ framework.

In this paper we describe the synthesis and properties of the novel polyspirocyclopolysilanes, $[(CH_2)_4Si]_n$, where n = 5–12, and $[(CH_2)_5Si]_n$, where n = 4–6.[7] These cyclosilanes are the first examples of rotane structures based on a ring of silicon atoms. Several of the properties of the silicon rotanes are unique among the cyclopolysilanes, probably due to the unusual steric effects of the cyclopolymethylene substituents. The X-ray crystal

(1) (a) West, R.; Carberry, E. *Science (Washington, D.C.)* **1975**, *189*, 179. (b) West, R. In "Comprehensive Organometallic Chemistry"; Wilkinson, G., Ed.; Pergamon Press: Oxford, 1982; Chapter 9.4. (c) Hengge, E. In "Homoatomic Rings, Chains and Macromolecules of the Main Group Elements"; Rheingold, A., Ed.; Elsevier: Amsterdam, 1977; Chapter 9. (d) West, R. *Pure Appl. Chem.* **1982**, *54*, 1041.
(2) Brough, L. F.; West, R. *J. Am. Chem. Soc.* **1981**, *103*, 3049.
(3) Brough, L. F.; West, R. *J. Organomet. Chem.* **1980**, *194*, 139.
(4) $(Et_2Si)_n$: Carlson, C. W.; Matsumura, K.; West, R. *J. Organomet. Chem.* **1983**, *194*, C5. Carlson, C. W.; West, R. *Organometalics* **1983**, *2*, 1792.
(5) $(R_2Si)_5$: Watanabe, H.; Muraoka, T.; Kohara, Y.; Nagai, Y. *Chem. Lett.* **1980**, 735.
(6) $(i\text{-PrSi})_4$: Watanabe, H.; Muraoka, T.; Kageyama, M.; Nagai, Y. *J. Organomet. Chem.* **1981**, *216*, C45.
(7) Our preliminary results were communicated earlier: Carlson, C. W.; West, R.; Zhang, X.-H. *Organometallics* **1983**, *2*, 453.

0002-7863/84/1506-5521$01.50/0

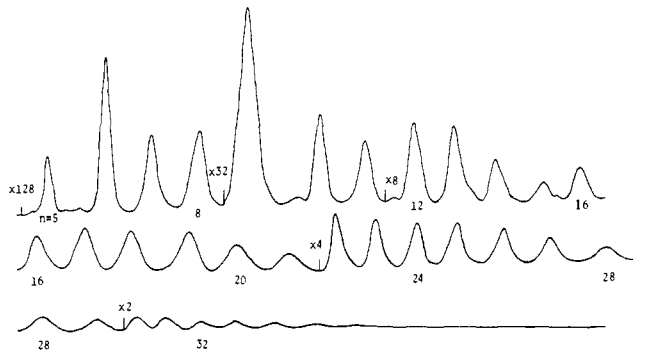

Figure 1. High-pressure liquid chromatogram of $[(CH_2)_4Si]_n$ cyclics, n = 5 to ca. 34, from the reaction of $(CH_2)_4SiCl_2$ and Li.

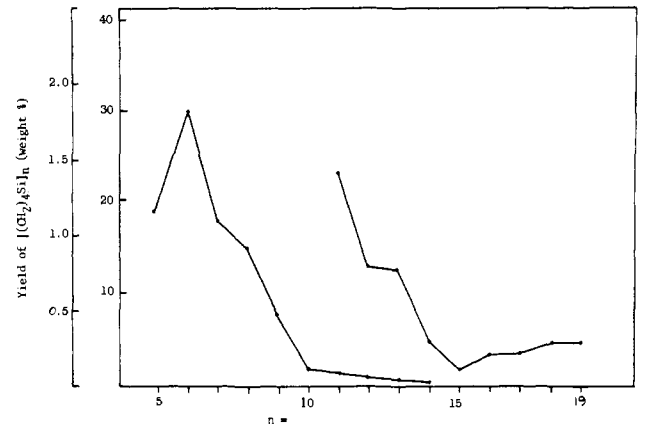

Figure 2. Weight % yields of $[(CH_2)_4Si]_n$ rotanes, n = 5–20, from reaction of $(CH_2)_4SiCl_2$ and Li; yields from n = 12 to 20 are estimated, see Experimental Section.

structures of cyclopentasilanes $[(CH_2)_4Si]_5$ (**1**) and $[(CH_2)_5Si]_5$ (**5**) are also described and discussed.

Results and Discussion

Synthesis of the Cyclotetramethylene Silicon Rotanes. The cyclotetramethylene cyclopolysilanes were made by reaction of alkali metals with cyclotetramethylenedichlorosilane $[(CH_2)_4SiCl_2]$; as for other cyclopolysilanes, such condensations produce mixtures of rings whose composition is dependent upon the reaction conditions.[7] Syntheses which promote equilibration among the cyclosilanes favor the thermodynamically most stable six-membered ring, **2**. Rings other than **2** are formed as kinetic products under nonequilibrium conditions. The preference for the cyclohexasilane is apparently related to the small size of the cyclotetramethylene substituent; by comparison, $(Me_2Si)_6$ is also the most stable oligomer among the methyl compounds,[3] while with substituents of greater bulk smaller ring sizes are favored (cf. $(Et_2Si)_5$[4] and $(t\text{-BuMeSi})_4$[8]).

The reaction of $(CH_2)_4SiCl_2$ with 2.0 equiv of Li in THF led to the formation of rotanes $[(CH_2)_4Si]_n$ of which those with n = 5–12 were isolated and characterized. HPLC analysis suggests that larger rings, up to about n = 34 in size, are also present, as shown in Figure 1. Similar nonequilibrium condensations using Li are known to form rings up to n = 35 in the $(Me_2Si)_n$ series.[2] There appears to be no marked preference for a single kinetic product in this reaction, unlike the condensations of Me_2SiCl_2 and Et_2SiCl_2 with 2.0 equiv of Li in which $(Me_2Si)_8$ and $(Et_2Si)_7$, respectively, are favored.[4,9]

A plot of the weight percent yields of $[(CH_2)_4Si]_n$ is shown in Figure 2. The rapid decrease in yield from n = 6 to 10 is thought to result from a medium-ring effect involving nonclassical strain, analogous to that known in carbocyclic chemistry.[10] The yields decrease more slowly after n = 10 and are approximately constant from n = 16 to 19, perhaps because the decreasing probability of ring closure (an entropy factor) is balanced by decreasing strain effects. The yields of large rings are greater if the chlorosilane is added rapidly to the lithium, evidently because the alkali metal is rapidly consumed; as a result, the Li-catalyzed equilibration among the rings is minimized.

Although condensations of dialkyldichlorosilanes with excess Li or excess potassium commonly give high yields of the thermodynamically favored cyclopolysilane, the analogous condensations of $(CH_2)_4SiCl_2$ led to quite different results. For example, a reaction of 2.2 equiv of Li and $(CH_2)_4SiCl_2$ in THF gave 2% $[(CH_2)_4Si]_5$ (**1**), 28% $[(CH_2)_4Si]_6$ (**2**), and a mixture consisting of 1% $[(CH_2)_4Si]_7$ (**3**) and 12% of a new compound to which we assign structure **3a**. Isomers **3** and **3a** could not be separated

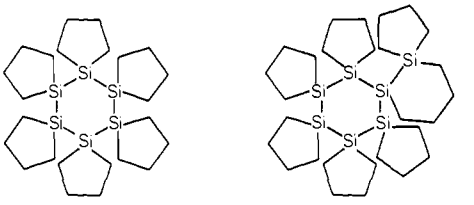

2 3a

by using either GLC or HPLC and were instead isolated as a mixture by HPLC. Reactions of $(CH_2)_4SiCl_2$ using either potassium or sodium–potassium alloy (Na/K) proceeded analogously and gave similar yields of **2**, **3**, and **3a**.

The structure assigned to **3a** is based mainly on its ^{29}Si NMR spectrum, which is similar to the known spectrum of (trimethylsilyl)undecamethylcyclohexasilane.[7,11] Rearrangement of this type is novel; cyclopolysilanes containing simple alkyl substituents do not undergo such rearrangement. The driving force for the reaction is probably the relief of steric strain when a silacyclopentane ring expands to the disilacyclohexane ring found in **3a**.[12]

High yields of **2** can be obtained by using short reaction times and conditions that favor rapid equilibration. Addition of $Ph_3SiSiMe_3$ as an equilibration agent[13] in a reaction of $(CH_2)_4SiCl_2$ and 2.2 equiv of Li in THF at 0 °C gave, after 5 h, a mixture of **2** (80%), **1** (1%), and **3** (4%), from which 68% of pure **2** could be isolated by recrystallization.

Synthesis of the Cyclopentamethylene Silicon Rotanes. The cyclopentamethylene compounds $[(CH_2)_5Si]_n$, where n = 4–6, were synthesized by the reaction of cyclopentamethylenedichlorosilane $[(CH_2)_5SiCl_2]$ with alkali metals.[14] The best yields of cyclopentamethylene rotanes were obtained by the reaction of $(CH_2)_5SiCl_2$ and 2.2 equiv of potassium in THF; after extended refluxing (54 h), yields of 64% $[(CH_2)_5Si]_5$ (**5**) and 16% $[(CH_2)_5Si]_6$ (**6**) were obtained. Shorter reaction times gave lower yields, evidently due to incomplete equilibration of polymers to the cyclopolysilanes. Cyclopentasilane **5** appears to be the thermodynamically favored ring among these compounds, consistent with the greater steric bulk of the cyclopentamethylene group compared to methyl and cyclotetramethylene substituents.

Condensations using only 2.0 equiv of potassium are known to give nonequilibrium distributions of cyclic products for both Me_2SiCl_2 and Et_2SiCl_2.[4] This was also observed for $(CH_2)_5SiCl_2$,

(8) Helmer, B. J.; West, R. *Organometallics*, **1982**, *1*, 1458.
(9) Matsumura, K.; Brough, L. F.; West, R. *J. Chem. Soc., Chem. Commun.* **1978**, 1092.
(10) For examples, see: Eliel, E. L.; Allinger, N. L.; Angyal, S. J.; Morrison, G. A. "Conformational Analysis"; Wiley: New York, 1965; Chapter 4.
(11) Ishikawa, M.; Watanabe, M.; Iyoda, J.; Ikeda, H.; Kumada, M. *Organometallics* **1982**, *1*, 317.
(12) For example, see: Cartledge, F. K. *J. Organomet. Chem.* **1982**, *225*, 131. Sommer, L. H.; Bennett, O. F. *J. Am. Chem. Soc.* **1959**, *81*, 251. Sommer, L. H.; Bennett, O. F.; Campbell, P. G.; Weyenberg, D. R. *Ibid.* **1957**, *79*, 3295.
(13) Chen, S.-M.; David, L. D.; Haller, K. J.; Wadsworth, C. L.; West, R. *Organometallics* **1983**, *2*, 409.
(14) These reactions proceed somewhat differently from those of either $(CH_2)_4SiCl_2$ and of other dialkyldichlorosilanes, perhaps as a consequence of the low reactivity of cyclopentamethylene-containing silanes. See: West, R. *J. Am. Chem. Soc.* **1954**, *76*, 6015.

Table I. NMR Data for Cyclotetramethylene and Cyclopentamethylene Rotanes

n	^{13}C,[a,b] ppm	^{29}Si,[a] ppm
	$[(CH_2)_4Si]_n$	
5	9.50, 29.70	−29.85
6	10.43, 29.81	−29.37
7	11.17, 29.86	−29.85
8	11.93, 29.91	−28.68
9	12.52, 29.84	−26.50
10	12.70, 29.84	−23.91
11	12.70, 29.86	−24.58
12	12.77, 29.91	−24.80
	$[(CH_2)_5Si]_n$	
4	10.40, 27.63, 30.56	−26.69
5	10.49, 27.27, 30.58	−42.91
6	11.32, 26.50, 30.14[c]	−42.58[c]

[a] In C_6D_6. [b] Intensity ratio is 1:1 for $[(CH_2)_4Si]_n$ and 2:2:1 for $[(CH_2)_5Si]_n$. [c] In $CDCl_3$.

although relatively small amounts of cyclopolysilanes were obtained. Yields were 19% **5**, 2% **6**, and 8% $[(CH_2)_5Si]_4$, **4**. Cyclotetrasilane **4** is also observed in the early stages of reactions of $(CH_2)_5SiCl_2$ with excess potassium, and appears, like $(Et_2Si)_4$, to be a kinetic product.

The reaction of Li and $(CH_2)_5SiCl_2$ proceeded well only under conditions in which the deactivation of the Li metal was minimized. Thus, the reaction of $(CH_2)_5SiCl_2$ using Li powder and sonication of the reaction solution formed 49% **5** and 5% **6**.[15] Condensation of $(CH_2)_5SiCl_2$ using sodium metal in refluxing toluene afforded moderate yields of **5** (35%) and **4** (10%).

Physical and Spectroscopic Properties. General. Cyclopentasilane **1** and to a lesser extent **2** are mildly oxygen-sensitive, in contrast to $(Me_2Si)_5$, which oxidizes only slowly, and unreactive $(Me_2Si)_6$. The remaining cyclotetramethylene compounds are stable in air. The reactivity of these rotanes appears to be generally higher than for other alkylcyclopolysilanes, consistent with the rather small steric protection provided by the cyclotetramethylene group. Rotanes **5** and **6** are both air stable and were purified by recrystallization; the cyclotetrasilane **4** is mildly susceptible to oxidation, much as is $(Et_2Si)_4$.[4]

Melting Points and Crystallinity. All of the silicon rotanes form colorless crystals (except for **4**, a colorless oil) which are considerably less soluble and less volatile than analogous acyclic alkylcyclopolysilanes. The cyclopentasilanes **1** and **5** have sharp, rather low melting points (90 and 110 °C, respectively), but the larger rings melt over broad ranges at higher temperatures. The silicon rotanes in the $[(CH_2)_4Si]_n$ series show large differences in their melting points with changes in ring size. Such variations probably result, at least in part, from the dependence of the crystal packing forces on the size and conformation of the ring. Similarly marked changes are also observed for the cycloalkanes, although the trends are somewhat different.

Both $(Me_2Si)_5$ and $(Me_2Si)_6$ are known to show plastic crystalline behavior.[16a] Cyclopentasilane $(Me_2Si)_5$ exists in the plastic state above −39 °C and exists as sticky, waxy-appearing crystals at ambient temperatures. Similarly, waxy crystals are formed by other cyclopentasilanes, including $(Et_2Si)_5$, $(n\text{-}Bu_2Si)_5$, and *cyclo*-$Si_5Me_9(SiMe_3)$, which probably adopt plastic crystalline phases at room temperature. By contrast, both **1** and **5** are isolated as well-defined crystals, and the absence of a plastic crystalline state at room temperature is shown by the fact that crystals of these compounds are suitable for X-ray diffraction study. The apparent crystallinity of **1** and **5**, and the low volatility of the silicon rotanes in general, probably results from the greater rigidity of the cyclopolymethylene substituents, which may promote more favorable packing and stronger intermolecular forces in the crystalline state.

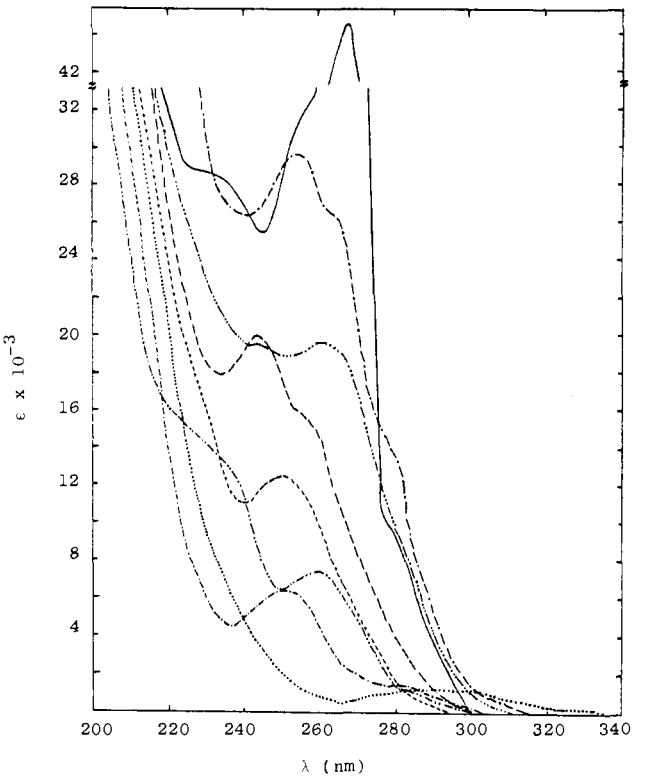

Figure 3. Ultraviolet absorption spectra of $[(CH_2)_4Si]_n$, n = 5 to 12 (5, ···; 6, - - -; 7, - · - ·; 8, - - -; 9, – – –; 10, —; 11, - · - · -; 12, – · · · – · · ·).

Nuclear Magnetic Resonance. The ^{13}C and ^{29}Si NMR data for the $[(CH_2)_4Si]_n$ and $[(CH_2)_5Si]_n$ compounds are given in Table I. The spectra indicate that the various environments in each of these rings are averaged by rapid interconversion among conformers. In the ^{13}C spectra of the cyclotetramethylene rotanes, two lines in 1:1 ratio are observed; the upfield line is assigned to the α-carbon and the downfield line to the β-carbon, on the basis of the expected shielding effect of silicon. The ^{29}Si NMR chemical shifts, which lie between −23 and −30 ppm for the $[(CH_2)_4Si]_n$ rings, are similar in magnitude to those of the ethyl-substituted cyclopolysilanes. The ^{29}Si and ^{13}C resonances all shift downfield with increasing ring size, most noticeably for the silicon and α-carbon resonances. Similar trends have been observed for the $(Et_2Si)_n$[4] and $(Me_2Si)_n$[2] cyclics. After about n = 10, the differences in the NMR shifts among adjacent rings are small, probably because conformational effects are less important as the rings become more like linear polysilanes in character.

The ^{13}C spectra of the cyclopentamethylene compounds show the expected 2:2:1 pattern, with the upfield resonances assigned to the α-carbons. The ^{29}Si NMR of **5** and **6** show resonances at about −43 ppm, quite different from the ethyl- and cyclotetramethylene-substituted rings, but resembling methyl compounds such as $(Me_2Si)_5$ and $(Me_2Si)_6$, which exhibit NMR peaks at −41.9 and −42.1 ppm, respectively.[2] The ^{29}Si signal of **4** is deshielded about 16 ppm relative to the larger rings; similar downfield shifts are observed in other strained cyclotetrasilanes as well.

The rearranged cyclohexasilane **3a** shows 11 lines in the ^{13}C spectrum, consistent with the variety of environments expected to be present. The lines from 10.4 to 17.8 ppm are assigned to the α-carbons, and those from 27.4 to 29.9 are assigned to the β-carbons.

Ultraviolet Spectra. The ultraviolet spectra of the $[(CH_2)_4Si]_n$ compounds are shown in Figure 3. The spectra of the cyclotetramethylene cyclopolysilanes show regular changes up to n = 10, which contains an anomalously intense band at 268 nm. This discontinuity is similar to the one observed at $(Me_2Si)_{10}$ in the methyl series of rings and may be related to sharp conformational

(15) Ultrasound-promoted reactions of Li with chlorosilanes have been previously reported. See, for example: Boudjouk, P.; Byung, H. H. *Tetrahedron Lett.* **1981**, *22*, 3813.

(16) (a) Larsen, D. W.; Soltz, B. A.; Stary, F. E.; West, R. *J. Phys. Chem.* **1980**, *84*, 1340. (b) The GC peak for this compound has the same retention time as **3** or **3a**. In the early stages of the rearranement this product may reasonably be assigned to **3** alone, as the formation of **3a** is observed to be slow.

changes in the medium-ring region in both series. The rearrangement product, **3a**, has a spectrum resembling that of **2** with λ_{max} at 270 and 245 nm.

Rearrangement of 2 and 3. In order to study the origin of the unusual rearrangement product **3a**, reactions of **2** and **3** with Ph_3SiLi as an equilibrating agent were carried out. The reaction of **2** and Ph_3SiLi in THF at 25 °C formed a mixture of 45% **2**, 3% **1**, and 40% of isomers **3** and **3a** after 72 h. A similar experiment using **3** formed 33% **2**, 5% **1**, and 32% of isomers **3** and **3a** after 30.5 h. In each case, the ^{13}C spectrum of the purified isomeric mixture confirmed the presence of **3** and established at **3**:**3a** ratio of about 1:15.

The reactions of Ph_3SiLi and **2** or **3** occur in two steps. The first is largely complete in the first hour of stirring; the solution at this point consists of about 86% **2**, 7% of **1**, and 7% of a third product, presumably **3**.[16b] This probably corresponds to the approximate equilibrium mixture of $[(CH_2)_4Si]_n$ rings.

The second step in the Ph_3SiLi-promoted rearrangement appears to be the slow formation of **3a**. The yield of the product assigned to isomers **3** and **3a** increases slowly, reaching a maximum after 2–3 days; NMR analysis then confirmed that the isomer mixture contained mainly **3a**.

The rearrangement to **3a** takes place under conditions which normally lead only to ring–ring redistribution in the cyclopolysilanes. The rearrangement does not require the **3a** form directly from **3**, since branched structures containing more or less than six silicons in the polysilane ring would be subsequently equilibrated to **3a**.[17]

The reaction does not appear to proceed thermally, but attempts to induce thermal rearrangement led to an unexpected redistribution of ring sizes. Pyrolysis of **2** (neat, in an evacuated sealed tube) at 220 °C for 3 days gave **1** (15%), **3** (5%), and unreacted **2** (80%), and identical pyrolysis of **3** formed 2% **1**, 3% **2**, and 95% recovered **3**. Additional attempts gave similar results. Thermal redistribution of cyclopolysilanes has not been previously reported, although a related process by which $(Me_2Si)_5$ and $(Me_2Si)_6$ are formed by heating dimethylsilylene polymer is known.[18] By comparison, the pyrolysis of $(Me_2Si)_6$ produced only small amounts of $(Me_2Si)_5$ and no $(Me_2Si)_7$.

Photolysis. Photolysis of **2** and **5** at 254 nm leads to ring contraction and concurrent extrusion of cyclotetramethylenesilylene $[(CH_2)_4Si]$ and cyclopentamethylenesilylene $[(CH_2)_5Si]$, respectively.[19] The silylene $(CH_2)_4Si$ has been obtained by a somewhat different route,[21] while $(CH_2)_5Si$ has not been previously reported.

When **5** was photolyzed in isooctane for 1.0 h, yields of 50% **4** and 32% recovered **5** were obtained. From such mixtures, pure **4** was isolated by preparative GLC. Carrying out the photolysis for 1.5 h in the presence of excess Et_3SiH, a known trapping agent for silylenes, gave high yields of $Et_3Si[(CH_2)_5Si]H$ and $Et_3Si[(CH_2)_5Si][(CH_2)_5Si]H$. An analogous photolysis using **2** and Et_3SiH in cyclohexane yielded 39% **1**, 42% **2**, 76% $Et_3Si(CH_2)_4SiH$, and 15% $Et_3Si(CH_2)_4Si(CH_2)_4SiH$ after 0.25 h. Small amounts of $[(CH_2)_4Si]_4$ may also be formed in the latter photolysis, but only its oxides are isolated.

Crystal Structures of 1 and 5. The spectroscopic and chemical properties of cyclopentasilanes have been closely studied,[1] but structural information on such molecules is rather limited. The crystal structure of $(Ph_2Si)_5$ has been determined,[22] and the structure of $(H_2Si)_5$ has been studied by electron diffraction.[23]

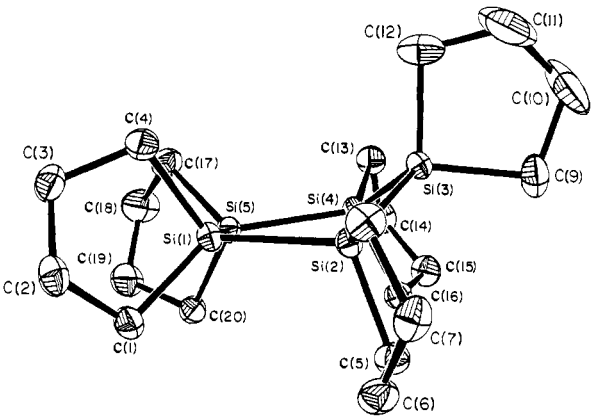

Figure 4. ORTEP drawing of $[(CH_2)_4Si]_5$ showing the conformation of the Si_5 ring. Ellipsoids are drawn at the 50% probability level.

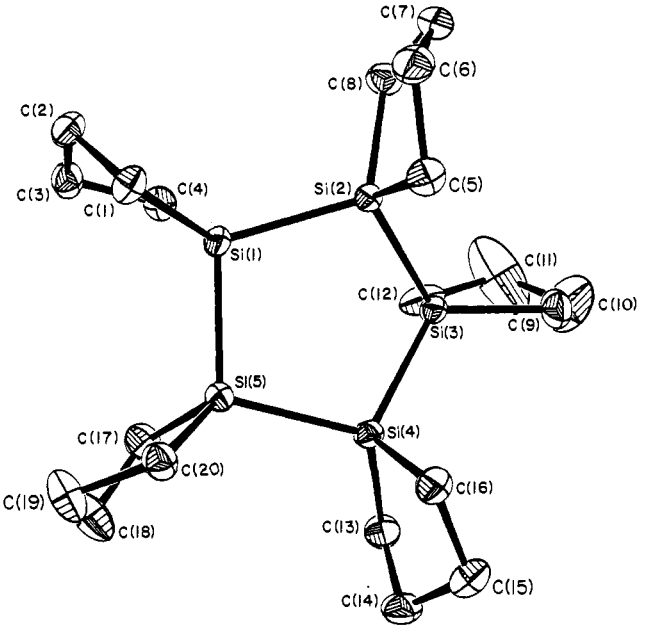

Figure 5. ORTEP drawing of $[(CH_2)_4Si]_5$ showing the conformations of the SiC_4 rings. Ellipsoids are drawn at the 50% probability level.

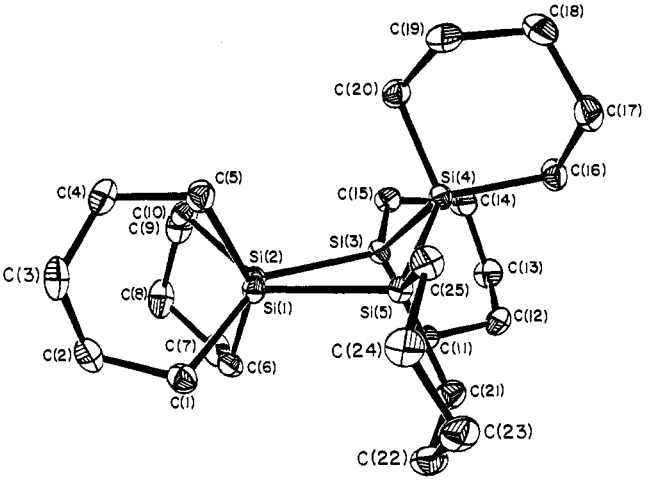

Figure 6. ORTEP drawing of $[(CH_2)_4Si]_5$ showing the conformations of the Si_4 rings. Ellipsoids are drawn at the 50% probability level.

An iron derivative of $(Me_2Si)_5$, *cyclo*-$Si_5Me_9(SiMe_2[Fe(CO)_2Cp])$ (**7**), has been examined by X-ray crystallography;[24] however, its structure does not appear to be strictly analogous to that for an unsubstituted ring.

(17) This is illustrated by the synthesis of *cyclo*-$Si_6Me_{11}(SiMe_3)$, which is made by rearrangement of *cyclo*-$Si_5Me_9(SiMe_3)$ in the presence of a catalytic amount of $PhMe_2SiLi$. See: Kumada, M.; Ishikawa, M.; Sakamoto, S.; Maeda, S. *J. Organomet. Chem.* **1969**, *17*, 223.

(18) Carberry, E.; West, R. *J. Am. Chem. Soc.* **1969**, *61*, 5440.

(19) Similar photolyses are well-known for other cyclopolysilanes, including $(Me_2Si)_6$[20] and $(Et_2Si)_7$.[4]

(20) Ishikawa, M.; Kumada, M. *J. Organomet. Chem.* **1972**, *42*, 325.

(21) Sakurai, H.; Kabayashi, Y.; Nakadaira, Y. *J. Am. Chem. Soc.* **1971**, *93*, 5272.

(22) Párkányi, L.; Sasvári, K.; Declercq, J. P.; Germain, G. *Acta Crystallogr., Sect. B* **1978**, *B34*, 3678.

(23) Smith, Z.; Seip, H. M.; Hengge, E.; Bauer, G. *Acta Chem. Scand., Ser A* **1976**, *A30*, 697.

(24) Drahnak, T. J.; West, R.; Calabrese, J. C. *J. Organomet. Chem.* **1980**, *198*, 55.

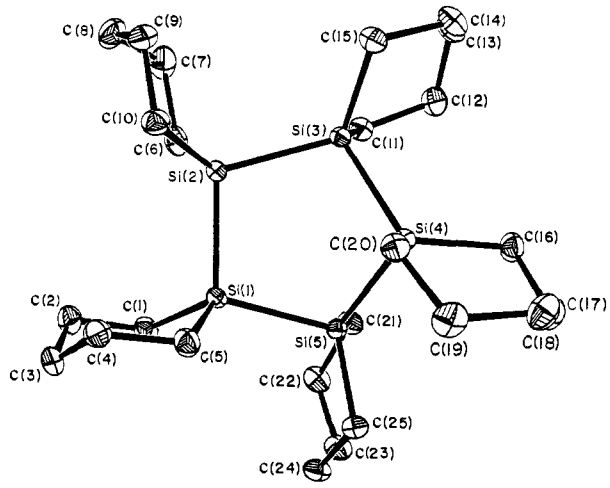

Figure 7. ORTEP drawing of $[(CH_2)_5Si]_5$ showing the conformations of the SiC_5 rings. Ellipsoids are drawn at the 50% probability level.

Table II. Selected Interatomic Distances (Å) for $[(CH_2)_4Si]_5$ (**1**)

Si–Si distances		C–C distances	
Si(1)–Si(2)	2.343 (1)	C(1)–C(2)	1.536 (2)
Si(2)–Si(3)	2.345 (1)	C(3)–C(4)	1.538 (2)
Si(3)–Si(4)	2.345 (1)	C(5)–C(6)	1.535 (3)
Si(4)–Si(5)	2.350 (1)	C(7)–C(8)	1.542 (3)
Si(5)–Si(1)	2.350 (1)	C(9)–C(10)	1.531 (4)
		C(11)–C(12)	1.463 (4)
Si–C distances		C(13)–C(14)	1.541 (3)
Si(1)–C(1)	1.910 (2)	C(15)–C(16)	1.540 (3)
Si(1)–C(1)	1.906 (2)	C(17)–C(18)	1.530 (3)
Si(2)–C(5)	1.903 (2)	C(19)–C(20)	1.540 (3)
Si(2)–C(8)	1.912 (2)		
Si(3)–C(9)	1.903 (2)	C(2)–C(3)	1.527 (3)
Si(3)–C(12)	1.900 (2)	C(6)–C(7)	1.533 (3)
Si(4)–C(13)	1.903 (2)	C(10)–C(11)	1.448 (6)
Si(4)–C(16)	1.910 (2)	C(14)–C(15)	1.516 (3)
Si(5)–C(17)	1.906 (2)	C(18)–C(19)	1.513 (3)
Si(5)–C(20)	1.910 (2)		

Table III. Selected Intramolecular Angles (deg) for $[(CH_2)_4Si]_5$ (**1**)

Si–Si–Si angles		C–Si–C angles	
Si(1)–Si(2)–Si(3)	103.98 (2)	C(1)–Si(1)–C(4)	94.80 (8)
Si(2)–Si(3)–Si(4)	101.29 (2)	C(5)–Si(2)–C(8)	94.50 (8)
Si(3)–Si(4)–Si(5)	106.25 (2)	C(9)–Si(3)–C(12)	94.51 (10)
Si(4)–Si(5)–Si(1)	105.55 (2)	C(13)–Si(4)–C(16)	94.69 (8)
Si(5)–Si(1)–Si(2)	105.50 (2)	C(17)–Si(5)–C(20)	94.46 (8)
Si–Si–C angles		Si–C–C angles	
Si(1)–Si(2)–C(5)	111.70 (6)	Si(1)–C(1)–C(2)	104.17 (11)
Si(1)–Si(2)–C(8)	113.87 (6)	Si(1)–C(4)–C(3)	102.67 (11)
Si(3)–Si(2)–C(5)	111.37 (6)	Si(2)–C(5)–C(6)	102.37 (12)
Si(3)–Si(2)–C(8)	121.40 (6)	Si(2)–C(8)–C(7)	104.59 (12)
Si(2)–Si(3)–C(9)	114.72 (7)	Si(3)–C(9)–C(10)	103.83 (18)
Si(2)–Si(3)–C(12)	116.56 (7)	Si(3)–C(12)–C(11)	104.29 (19)
Si(4)–Si(3)–C(9)	115.26 (8)	Si(4)–C(13)–C(14)	102.60 (12)
Si(4)–Si(3)–C(12)	115.43 (7)	Si(4)–C(16)–C(15)	103.93 (12)
Si(3)–Si(4)–C(13)	118.28 (6)	Si(5)–C(17)–C(18)	103.74 (13)
Si(3)–Si(4)–C(16)	111.71 (6)	Si(5)–C(20)–C(19)	103.87 (13)
Si(5)–Si(4)–C(13)	115.06 (6)		
Si(5)–Si(4)–C(16)	110.49 (6)	C–C–C angles	
Si(1)–Si(5)–C(17)	113.20 (7)	C(1)–C(2)–C(3)	109.36 (14)
Si(1)–Si(5)–C(20)	114.48 (6)	C(2)–C(3)–C(4)	108.50 (14)
Si(4)–Si(5)–C(17)	115.67 (7)	C(5)–C(6)–C(7)	108.09 (15)
Si(4)–Si(5)–C(20)	113.68 (6)	C(6)–C(7)–C(8)	109.70 (14)
Si(5)–Si(1)–C(1)	113.23 (6)	C(9)–C(10)–C(11)	113.44 (23)
Si(5)–Si(1)–C(4)	112.07 (6)	C(10)–C(11)–C(12)	114.9 (3)
Si(2)–Si(1)–C(1)	118.22 (6)	C(13)–C(14)–C(15)	108.16 (15)
Si(2)–Si(1)–C(4)	113.06 (6)	C(14)–C(15)–C(16)	109.56 (15)
		C(17)–C(18)–C(19)	109.70 (18)
		C(18)–C(19)–C(20)	108.82 (17)

Crystals of **1** and **5** were grown by vapor diffusion, and structures of the two compounds were determined by X-ray diffraction. Both molecules adopted a conformation intermediate between C_s (envelope) and C_2 (half-chair). The structure of **1** is shown in Figures 4 and 5, and similar views of **5** are given in Figures 6 and 7. Bond distances and bond angles are shown in Tables II and III for **1** and in Tables IV and V for **5**.

Table IV. Selected Interatomic Distances (Å) for $[(CH_2)_5Si]_5$ (**5**)

Si–Si distances		C–C distances	
Si(1)–Si(2)	2.363 (1)	C(1)–C(2)	1.540 (2)
Si(2)–Si(3)	2.366 (1)	C(4)–C(5)	1.534 (2)
Si(3)–Si(4)	2.354 (1)	C(6)–C(7)	1.536 (2)
Si(4)–Si(5)	2.360 (1)	C(9)–C(10)	1.531 (2)
Si(5)–Si(1)	2.350 (1)	C(11)–C(12)	1.536 (2)
		C(14)–C(15)	1.540 (2)
Si–C distances		C(16)–C(17)	1.541 (2)
Si(1)–C(1)	1.894 (1)	C(19)–C(20)	1.538 (2)
Si(1)–C(5)	1.897 (1)	C(21)–C(22)	1.541 (2)
Si(2)–C(6)	1.890 (1)	C(24)–C(25)	1.534 (2)
Si(2)–C(10)	1.892 (1)		
Si(3)–C(11)	1.894 (1)	C(2)–C(3)	1.524 (2)
Si(3)–C(15)	1.894 (1)	C(3)–C(4)	1.527 (2)
Si(4)–C(16)	1.894 (1)	C(7)–C(8)	1.523 (2)
Si(4)–C(20)	1.896 (1)	C(8)–C(9)	1.526 (2)
Si(5)–C(21)	1.896 (1)	C(12)–C(13)	1.525 (2)
Si(5)–C(25)	1.894 (1)	C(13)–C(14)	1.531 (2)
		C(17)–C(18)	1.527 (2)
		C(18)–C(19)	1.526 (2)
		C(22)–C(23)	1.531 (2)
		C(23)–C(24)	1.532 (2)

Table V. Selected Intramolecular Angles (deg) for $[(CH_2)_5Si]_5$ (**5**)

Si–Si–Si angles		Si–C–C angles	
Si(1)–Si(2)–Si(3)	105.70 (2)	Si(1)–C(1)–C(2)	110.42 (9)
Si(2)–Si(3)–Si(4)	102.11 (2)	Si(1)–C(5)–C(4)	112.32 (9)
Si(3)–Si(4)–Si(5)	100.17 (2)	Si(2)–C(6)–C(7)	110.90 (9)
Si(4)–Si(5)–Si(1)	99.94 (2)	Si(2)–C(10)–C(9)	111.38 (9)
Si(5)–Si(1)–Si(2)	104.56 (2)	Si(3)–C(11)–C(12)	110.90 (8)
		Si(3)–C(15)–C(14)	110.68 (9)
Si–Si–C angles		Si(4)–C(16)–C(17)	110.97 (8)
Si(1)–Si(2)–C(6)	112.25 (5)	Si(4)–C(20)–C(19)	111.84 (8)
Si(1)–Si(2)–C(10)	113.85 (4)	Si(5)–C(21)–C(22)	110.59 (8)
Si(3)–Si(2)–C(6)	107.08 (4)	Si(5)–C(25)–C(24)	110.82 (8)
Si(3)–Si(i)–C(10)	115.05 (4)		
Si(2)–Si(3)–C(11)	109.34 (4)	C–C–C angles	
Si(2)–Si(3)–C(15)	118.13 (4)	C(1)–C(2)–C(3)	112.94 (11)
Si(4)–Si(3)–C(11)	110.96 (4)	C(3)–C(4)–C(5)	113.59 (11)
Si(4)–Si(3)–C(15)	115.04 (4)	C(6)–C(7)–C(8)	113.32 (11)
Si(3)–Si(4)–C(16)	120.29 (4)	C(8)–C(9)–C(10)	113.41 (11)
Si(3)–Si(4)–C(20)	109.14 (4)	C(11)–C(12)–C(13)	113.46 (11)
Si(5)–Si(4)–C(16)	114.36 (4)	C(13)–C(14)–C(15)	113.39 (11)
Si(5)–Si(4)–C(20)	110.68 (4)	C(16)–C(17)–C(18)	114.03 (11)
Si(4)–Si(5)–C(21)	113.51 (4)	C(18)–C(19)–C(20)	113.25 (11)
Si(4)–Si(5)–C(25)	117.46 (4)	C(21)–C(22)–C(23)	114.08 (11)
Si(1)–Si(5)–C(21)	112.65 (4)	C(23)–C(24)–C(25)	113.13 (10)
Si(1)–Si(5)–C(25)	110.53 (4)		
Si(5)–Si(1)–C(1)	119.83 (4)	C(2)–C(3)–C(4)	114.43 (10)
Si(5)–Si(1)–C(5)	107.80 (4)	C(7)–C(8)–C(9)	113.82 (11)
Si(2)–Si(1)–C(1)	110.38 (4)	C(12)–C(13)–C(14)	114.73 (11)
Si(2)–Si(1)–C(5)	112.61 (4)	C(17)–C(18)–C(19)	114.30 (11)
		C(22)–C(23)–C(24)	114.14 (10)
C–Si–C angles			
C(1)–Si(1)–C(5)	101.85 (6)		
C(6)–Si(2)–C(10)	102.87 (6)		
C(11)–Si(3)–C(15)	101.39 (5)		
C(16)–Si(4)–C(20)	102.28 (6)		
C(21)–Si(5)–C(25)	103.11 (6)		

The Si–Si–Si bond angle ranges from 101.3° to 106.3° in **1** and averages 104.5 (20)°, similar to the average in $(H_2Si)_5$ (104.3°) and $(Ph_2Si)_5$ (104.5°). The corresponding average in **5** is a somewhat smaller 102.5 (26)°, and ranges from 99.9° to 105.7°. The average C–Si–C angles are markedly compressed in both compounds relative to cyclosilanes bearing acyclic substituents. It is 102.3 (7)° for **5** and only 94.6 (2)° for **1**. Comparable values for related compounds are $(Ph_2Si)_5$, 105.9°; $(H_2Si)_5$ (H–Si–H angle), 105.3°; **7**, 108.2°; $(Me_2Si)_6$, 108.1°;[25] and (*t*-

(25) Carrell, H. L.; Donohue, J. *Acta Crystallogr., Sect. B* **1972**, *B28*, 1566.

Table VI. Torsional Angles of $[(CH_2)_4Si]_5$ (1) and $[(CH_2)_5Si]_5$ (5)

	torsional angles, deg			
	$[(CH_2)_4Si]_5$		$[(CH_2)_4Si]_5$	
atoms	meas	calcd[a]	meas	calcd[b]
Si(1)–Si(2)–Si(3)–Si(4)	41.7	41.7	22.0	22.1
Si(2)–Si(3)–Si(4)–Si(5)	−35.9	−35.6	−45.6	−45.6
Si(3)–Si(4)–Si(5)–Si(1)	16.5	16.1	51.7	51.7
Si(4)–Si(5)–Si(1)–Si(2)	9.7	9.6	−37.9	−38.1
Si(5)–Si(1)–Si(2)–Si(3)	−32.3	−31.7	10.0	9.9

[a] Using $\Delta = -9.3$ and $\phi_m = 41.7$; see ref 27. [b] Using $\Delta = -14.1$ and $\phi_m = 52.1$; see ref 27.

Table VII. Comparison of the Average Parameters of the SiC_5 Rings in $[(CH_2)_5Si]_5$ (5) with Silacyclohexane

parameters[c]	$[(CH_2)_5Si]_5$	SiC_5H_{12}[a,b]
Si–C dist, Å	1.894 (2)	1.885
C_1–C_2 dist, Å	1.537 (3)	1.550
C_2–C_3 dist, Å	1.527 (3)	
C–Si–C angle, deg	102.3 (7)	104.2
Si–C–C angle, deg	111.1 (6)	110.6
C_1–C_2–C_3 angle, deg	113.5 (4)	113.7
C_2–C_3–C_4 angle, deg	114.3 (3)	111.4
τ_{Si-C}	46.1 (15)	44.0
$\tau_{C_1-C_2}$	56.9 (14)	57.3
$\tau_{C_2-C_3}$	65.1 (12)	67.5

[a] Electron diffraction data; see ref 30. [b] C_s conformation. [c] Numbered so that C_1 and C_5 are adjacent to the silicon.

BuMeSi)$_4$, 107.4°.[26] The small C–Si–C angles, leading to decreased steric protection for the Si–Si bonds, undoubtedly contributes to the high reactivity observed for cyclics in the $[(CH_2)_4Si]_n$ series.

The Si–Si bond lengths in the two rotanes are 2.359 (7) Å for **5** and 2.347 (3) Å for **1**. The longer value for **5** probably results from greater steric repulsions for cyclopentamethylene groups relative to the cyclotetramethylene groups in **1**. By comparison, the crowded $(Ph_2Si)_5$ has an Si–Si distance of 2.396 Å, among the longest Si–Si length yet reported. The Si–Si distance in unsubstituted $(H_2Si)_5$, 2.342 Å, resembles the bond length in **1**, again suggesting that the steric effect of the cyclotetramethylene substituent is small.

The torsional angles present in the central silicon rings of the cyclopentasilanes are given in Table VI. Following the method of Altona, Geise, and Romers.[27,28] the distortion of the Si_5 ring from C_2 and C_5 symmetry was determined. The pseudorotation phase angle, Δ, was found to be −9.3° for **1** and −14.1° for **5**, where Δ is zero in the case of C_2 symmetry and −36° for C_s symmetry. Hence, the degree of distortion is similar for the two compounds and resembles $(Ph_2Si)_5$, for which the Δ value was found to be −15.9. The pseudorotation model was found to fit both cyclosilanes; the angles calculated by using the derived Δ value are shown in Table VI and closely correspond to the measured angles.

The average of the torsional angles (absolute values) has been suggested to be a measure of the degree of planarity in a cyclic molecule.[29] This average is 33.4° for **5** and a somewhat smaller 27.2° for **1**. By comparison, the average of the torsional angles is 27.0° for $(Ph_2Si)_5$, 27.7° for **7**, and for $(H_2Si)_5$, 26.7° (if C_s symmetry) or 27.9° (if C_2 symmetry). Hence **5** appears to be less planar than other known cyclopentasilanes. This may result because steric interaction of the silacyclohexane groups in **5** is minimized at large torsional angles. The slightly greater steepness of the torsional angles in **5** is also demonstrated by comparison of the maximum torsion angle, ϕ_m, associated with the pseudorotation phase angle Δ. This value is 41.7° and 41.9° for **1** and $(Ph_2Si)_5$, respectively, but is 52.1° for **5**.

(26) Hurt, C. J.; Calabrese, J. C.; West, R. *J. Organomet. Chem.* **1975**, *91*, 273.
(27) Altona, C.; Geise, H. J.; Romers, C. *Tetrahedron* **1968**, *24*, 13.
(28) Eliel, E. L.; Allinger, N. L. "Topics in Stereochemistry"; Wiley: New York, 1974; Vol. 8, p 187.
(29) Bucont, R. "Topics in Stereochemistry"; Wiley: New York, 1974; Vol. 8, p 163.

Table VIII. Comparison of the Average Parameters of the SiC_4 Rings in $[(CH_2)_4Si]_5$ (1) with Silacyclopentane

parameters[c]	$[(CH_2)_4Si]_5$	SiC_4H_{10}[a,b]
Si–C dist, Å	1.906 (4)	1.892
C_1–C_2 dist, Å	1.537 (4)	1.535
C_2–C_3 dist, Å	1.522 (9)	1.580
C–Si–C angle, deg	94.6 (2)	96.3
Si–C–C angle, deg	103.6 (8)	103.6
C–C–C angle, deg	110 (2)	108.4
τ_{Si-C}		13.3
$\tau_{C_1-C_2}$		36.1
$\tau_{C_2-C_3}$		49.7

[a] Electron diffraction and microwave data; see ref 30. [b] C_2 conformation. [c] Numbered so that C_1 and C_4 are adjacent to the silicon.

Table IX. Magnitude of the SiC_4 Torsional Angles in $[(CH_2)_4Si]_5$ (1)

atoms	torsional angle, deg
Si(1)–C(1)–C(2)–C(3)	32.1
C(1)–C(2)–C(3)–C(4)	50.1
C(2)–C(3)–C(4)–Si(1)	41.0
C(3)–C(4)–Si(1)–C(1)	19.0
C(4)–Si(1)–C(1)–C(2)	6.8
Si(2)–C(5)–C(6)–C(7)	43.8
C(5)–C(6)–C(7)–C(8)	48.9
C(6)–C(7)–C(8)–Si(2)	27.6
C(7)–C(8)–Si(2)–C(5)	1.6
C(8)–Si(2)–C(5)–C(6)	23.7
Si(3)–C(9)–C(10)–C(11)	19.6
C(9)–C(10)–C(11)–C(12)	34.3
C(10)–C(11)–C(12)–Si(3)	29.4
C(11)–C(12)–Si(3)–C(9)	14.3
C(12)–Si(3)–C(9)–C(10)	2.3
Si(4)–C(13)–C(14)–C(15)	41.8
C(13)–C(14)–C(15)–C(16)	50.6
C(14)–C(15)–C(16)–Si(4)	32.1
C(15)–C(16)–Si(4)–C(13)	6.2
C(16)–Si(4)–C(13)–C(14)	19.7
Si(5)–C(17)–C(18)–C(19)	36.5
C(17)–C(18)–C(19)–C(20)	49.4
C(18)–C(19)–C(20)–Si(5)	35.7
C(19)–C(20)–Si(5)–C(17)	12.4
C(20)–Si(5)–C(17)–C(18)	13.0

Although both silacyclopentane $[H_2Si(CH_2)_4]$ and silacyclohexane $(H_2Si(CH_2)_5]$ have been studied by electron diffraction,[30] no crystal structures are known for either substituted or unsubstituted silacyclopentanes and silacyclohexanes. The silicon rotanes **1** and **5** are therefore the first compounds containing these heterocyclic rings to be studied by X-ray diffraction.

All of the silacyclohexane rings in **5** are quite similar to one another. Each is very close to a symmetrical chain (C_s) conformation and is flattened at the silicon end. A comparison of the average bond distances, bond angles, and torsional angles found in **5** with the corresponding values in $H_2Si(CH_2)_5$ is shown in Table VII. Although differences exist (e.g., smaller C–Si–C angles and less puckering at carbon C_3 in **5**), the structures appear to be remarkably similar.

The average bond distances and angles found in the silacyclopentane rings of **1** are shown in Table VIII, along with analogous values for the unsubstituted silacyclopentane. (One ring in **1**, Si(3)–C(9)–C(10),–C(11)–C(12), contained atoms with large thermal parameters, suggesting apparent disorder in the crystal. It gave anomalous distances and angles and was omitted in our determination of the averages.) The values for $H_2Si(CH_2)_4$ and **1** match rather closely, with the exception of a ca. 2° larger C–Si–C angle and a much larger C_2–C_3 distance in the $H_2Si(CH_2)_4$ structure.

(30) Shen, Q.; Hildebrandt, R. L.; Mastryukov, V. S. *J. Mol. Struct.* **1979**, *54*, 121.

The silacyclopentane rings in **1** exist in a number of different conformational states. This may be understood if the conformations along the pseudorotational pathway of silacyclopentane are similar in energy. In such a case, the geometries adopted by each of the rings would be influenced by the crystal packing forces. In the silacyclohexane rings of **5**, larger energy differences between the preferred chair form and other possible conformations (e.g., boat) are probably present. As a consequence, packing forces are less important in determining the ring geometry and only conformations close to the stable chair form are observed.

The torsional angles present in the five silacyclopentane rings of **1** are listed in Table IX. Each of these rings is intermediate in a conformation between the envelope and half-chair forms. The ring attached at Si(5) resembles the reported $H_2Si(CH_2)_4$ structure and is in an approximate C_2 conformation, while the Si(2) ring is a near envelope with the puckering at a β-carbon, C(6). The remaining silacyclopentane units of **1** adopt conformations falling between these two extremes. Although an apparent flattening is observed for the ring at Si(3), it probably results from the disorder observed to be present in this ring.

Experimental Section

Chlorosilanes $(CH_2)_4SiCl_2$ and $(CH_2)_5SiCl_2$ were prepared following the literature procedures.[14] Tetrahydrofuran (THF) was predried over KOH and distilled from sodium naphthalide. Toluene was refluxed over sodium for 12–24 h and then distilled. Preformed Na/K alloy (78% potassium by weight) was obtained from Callery Chemical Co. Analyses were completed by Galbraith Laboratories, Knoxville, TN. Syringe and Schlenk techniques were used in the handling of moisture-or oxygen-sensitive compounds. Yields were determined by analytical GLC using $C_{18}H_{38}$ or $C_{32}H_{66}$ as an internal standard, and the values were corrected for the different responses of the cyclosilanes and the standard on the detector.

GLC analyses on an analytical scale were done by using a Hewlett-Packard 5720A gas chromatograph equipped with a flame-ionization detector. The rather nonvolatile cyclopolysilanes were analyzed by using a 2.5 ft × $^1/_8$ in. Dexsil column (5% on Chromosorb W), and more volatile compounds were analyzed with longer (6 ft or 20 ft) SE-30 columns (20% on Chromosorb W). A Varian Model 90-P chromatograph containing a thermal conductivity detector and equipped with a 5 ft × $^3/_8$ in. SE-30 column (20% on Chromosorb W) was used for preparative GLC separations. HPLC separations were carried out by using two Waters Associates 6000 LC pumps, which were connected in series and equipped with an Altex model 153 UV detector (detection at 254 nm). Either a Whatman M-9 ODS-2 semipreparative column or a Whatman M-20 ODS-2 preparative column was used. The mobile phase consisted of MeOH and THF mixtures of various compositions and usually was programmed to vary from 70% MeOH and 30% THF to 50% MeOH and 50% THF.

NMR spectra were obtained by using C_6D_6 or $CDCl_3$ as solvents and Me_4Si as an internal standard. ^1H NMR spectra were determined on a JEOL MH-100 or a Brüker WP-200 spectrometer. ^{13}C NMR spectra were collected on either a JEOL FX-60 (15.04 MHz) or a JEOL FX-200 (50.10 MHz). All ^1H, ^{13}C, and ^{29}Si chemical shifts are referenced in parts per million. ^{29}Si NMR spectra were obtained on a JEOL FX-200 (39.60 MHz) using the INEPT method with delay times Δ = 25.7 ms and τ = 38.5 ms.[31] Mass spectra were obtained on a Kratos MS 9020 mass spectrometer at 70 eV. IR spectra were recorded on a Beckman 4250 IR spectrophotometer over the region 200–4000 cm^{-1}. UV spectra were obtained from 190 to 350 nm with a Cary 118 spectrophotometer using spectrograde 2,2,4-trimethylpentane. Values of λ and ϵ are reported in nm and M^{-1} cm^{-1}, respectively.

Synthesis of the Cyclotetramethylene Silicon Rotanes. 1. Reaction of $(CH_2)_4SiCl_2$ with 2.0 Equiv of Li. These reactions require degassed, peroxide-free THF and exclusion of air, since one product, **1**, is susceptible to oxidation. In a typical reaction, 0.22 g of Li wire (2.0 equiv, 32 mmol) and 50 mL of dry, freshly distilled THF were added to a 100-mL flask equipped with a mechanical stirrer and an argon inlet. The solution was degassed by using a stream of argon and cooled to 0 °C, and 2.5 g (16 mmol) of $(CH_2)_4SiCl_2$ was added dropwise over 2.2 h while the temperature was maintained at 0 °C. The mixture was stirred at this temperature for an additional 16 h, forming a colorless solution containing no unreacted Li. The lithium chloride was removed by two cycles consisting of concentration by distillation of the solvent under reduced pressure, filtration by cannulation of the solution through a glass wool plug, and addition of dry, degassed hexane. Evaporation of the solvent then left 1.36 g of a white, waxy solid containing the silicon rotanes $[(CH_2)_4Si]_n$. No polymer and only traces of minor products were detected. Yields (n, %): 5, 20; 6, 39; 7, 14; 8, 7.3; 9, 5.5; 10, 2.6; 11, 2.9; 12, 1.4. For n = 5–7 these were determined by using GLC analysis, while for n = 8–12 the yields were calculated from peak areas determined by HPLC, corrected for molecular weight and absorbance at the detection frequency, 254 nm. Yields for n = 13–19 (Figure 2) were estimated from the HPLC peak areas, using absorbances of the corresponding $(Me_2Si)_n$ rings.[2] Each of the cyclopolysilanes up to n = 12 was obtained as pure, colorless crystals by preparative HPLC. All of the compounds $[(CH_2)_4Si]_n$ gave similar mass spectra. A typical spectrum, including relative intensities and possible assignment, is shown for **2**: 507 (3.1, M + 3), 506 (10.8, M + 2), 505 (16.5, M + 1), 504 (32.7, M^+), 225 (0.7, $[(CH_2)_4]_2Si_2C_4H_9$), 169 (2.4, $[(CH_2)_4]Si_2H$), 113 (5.1, $[(CH_2)_4]SiC_2H_5$), 85 (29.5, $(CH_2)_4SiH$), 83 (37.9, $(C_4H_6)SiH$), 57 (59.8, C_4H_9), 55 (48.7, C_4H_7), 43 (100, C_3H_7), 41 (93.2, C_3H_5).

The ^1H NMR spectrum of each compound consisted of two indistinct multiplets in 1:1 ratio, appearing at about 0.70–1.20 and 1.50–1.90 ppm. Infrared spectra were also essentially identical above 600 cm^{-1}.

$[(CH_2)_4Si]_5$: mp 89.5–90 °C; IR 496 (vw, sh), 472 (w), 420 (w), 323 (m, br); UV [λ (ϵ)] 290 (1050) (probable doublet), 212 sh (33 000). Exact mass calcd 420.1965; obsd 420.1975, dev 2.4 ppm.

$[(CH_2)_4Si]_6$: mp 202–212 °C; IR 494 (w, sh), 474 (m), 416 (m), 308 (m); UV [λ (ϵ)] 279 sh (1200), 252 (5100), ~225 (8500), 208 sh (31 300). Exact mass calcd 504.2358; obsd 504.2370, dev 2.4 ppm. Anal. Calcd for $C_{24}H_{48}Si_6$: C, 57.06; H, 9.58; Si, 33.36. Found: C, 56.89; H, 9.41; Si, 33.20.

$[(CH_2)_4Si]_7$: mp 210–218 °C; IR 495 (w), 476 (m), 413 (w), 366 (w); UV [λ (ϵ)] 260 sh (5300), 236 sh (10 000). Exact mass calcd 588.2751; obsd 588.2764, dev 2.2 ppm. Anal. Calcd for $C_{28}H_{56}Si_7$: C, 57.06; H, 9.58. Found: C, 56.87; H, 9.66.

$[(CH_2)_4Si]_8$: dec >310 °C; IR 492 (m), 473 (m), 414 (m); UV [$\lambda(\epsilon)$] ~265 sh (7100), 254 (11 000), 228 sh (17 000). Exact mass calcd 672.3144; obsd 672.3165, dev 3.1 ppm.

$[(CH_2)_4Si]_9$: mp 156–162 °C; IR 492 (m), 475 (w, br), 415 (w), 380 (w); UV [λ (ϵ)] 264 sh (1200), 246 (20 000), 223(24 000). Exact mass calcd 756.3537; obsd: 756.3559, dev 2.9 ppm.

$[(CH_2)_4Si]_{10}$: dec 360 °C; IR 491 (m), 479 (w, br), 413 (m); UV [λ (ϵ)] 282 sh (8500), 268 (44 000), 225 sh (31 000), 237 (28 000). Exact mass calcd 840.3930; obsd 840.3951, dev 2.4 ppm.

$[(CH_2)_4Si]_{11}$: cloudy melt 170 °C, melts 194–200 °C; IR 493 (m), 473 (w, sh), 415 (m); UV [λ (ϵ)] ~283 sh (10 000), 268 (24 000), 254 (29 000), 235 sh (27 000). Exact mass calcd 924.4323; obsd 924.4350, dev 2.9 ppm.

$[(CH_2)_4Si]_{12}$: dec 360 °C; IR 489 (m), 470 (w, sh), 412 (w), 345 (w); UV [λ (ϵ)] ~283 sh (7700), 265 (19 000), 247 (19 000), 230 sh (23 000).

The speed of addition of the chlorosilane affects the products obtained in the reactions of $(CH_2)_4SiCl_2$ and 2.0 equiv of Li. When the chlorosilane is added over periods of 0.5, 1.0, and 1.5 h, in each case a colorless solution forms containing $[(CH_2)_4Si]_n$, where n = 5 to ca. 21–25. Very slow additions (~4 h) cause a blue color to appear and only cyclics from 5 to 15 are seen.

Rings up to 34 in size were obtained by the following modification: a stirred solution of 300 mL of dry THF and 1.38 g (0.20 mol) of Li was maintained at 0 °C and 15.5 g (0.10 mol) of $(CH_2)_4SiCl_2$ was added rapidly over a period of less than 1 min. After 2 h of stirring at 0 °C, the reaction was worked up as described previously and the product examined by HPLC (Figure 1). The yields of rings from n = 5 to n = 12 were determined by GLC and HPLC analysis as described above: n = 5, 19%; 6, 30; 7, 18; 8, 15; 9, 7.4; 10, 1.6; 11, 1.4; 12, 0.8.

The reaction of $(CH_2)_4SiCl_2$ (2.5 g, 16 mmol) and Li wire (0.24 g, 35 mmol) in 50 mL of dry THF at 0 °C was carried out as described previously.[4] After 12 h of stirring at 0 °C, the deep green solution (which reverted to colorless upon exposure to air) was worked up; GLC analysis showed the cyclosilanes to be present in yields of 2% **1**, 28% **2**, and 13% of a mixture of **3** and **3a**. No polymer or rings greater than seven in size were observed in this reaction. A number of minor, volatile products were also detected by GLC but were not examined closely. Isomers **3** and **3a** were not resolved by either analytical GLC or HPLC, giving a single, slightly broadened peak in each case. They were isolated as a mixture by HPLC and **3a** was identified by its ^{29}Si NMR (Table I), determined in C_6D_6 using $Cr(acac)_3$ as a paramagnetic relaxation agent. Measurement of the peak intensities showed the **3a**:**3** ratio to be 12:1, corresponding to a purity for **3a** of 92%. The mixture formed colorless crystals: mp 87–88 °C; UV [$\lambda(\epsilon)$] 270 sh (4600), 245 sh (10 500), 209 sh (44 400); ^{13}C NMR ($CDCl_3$) δ (relative intensity) 29.91 (5.1), 29.73 (6.7), 28.64 (1.7), 28.02 (2.8), 27.41 (1.3), 17.82 (1.5), 13.36 (2.2), 11.65 (5.7), 11.03 (1.0, $[(CH_2)_4Si]_7$), 10.73 (5.1), 10.51 (2.1); ^1H NMR (C_6D_6) δ 0.70–1.30 (m, 4 H), 1.40–1.90 (m, 4 H). Exact mass calcd 588.2751; obsd 588.2764, dev 2.2 ppm.

(31) Helmer, B. J.; West, R. *Organometallics* **1982**, *1*, 877.

The mass spectrum of **3a** resembles that of other tetramethylene silicon rotanes. The IR spectrum (4000–600 cm^{-1}) shows several additional bands when compared to pure **3**, and only C–H, C–C, and Si–C modes are present.

To form high yields of **2**, 7.8 g (50 mmol) of $(CH_2)_4SiCl_2$ was added over 1 h to a solution of 150 mL of dry THF, 0.76 g (110 mmol) of Li wire, and 20 mg of $Ph_3SiSiMe_3$. The solution was maintained at 0 °C. After 0.5 h, GLC showed cyclosilanes **1**, **2**, and **3** to be present in a 2:5:2 ratio. The deep green-brown solution was stirred for a total of 5 h at 0 °C; workup then gave 4.09 go of white crystals containing the cyclopolysilanes in yields of 80% **2**, 4% **3**, and 1% **1**. Another compound, eluted immediately before **2** on the GLC, was present in 4% yield. It was believed to be the oxide of **2**, *cyclo*-$[(CH_2)_4Si]_6O$, but was not isolated. Recrystallization of the product from EtOH/THF led to isolation of 2.9 g (68%) of pure **2**.

The reaction of $(CH_2)_4SiCl_2$ (7.8 g, 50 mmol) and potassium (4.3 g, 110 mmol) in 150 mL of dry, refluxing THF, following the usual procedure,[2,4] formed a deep green solution; after 16 h, the solution was quenched yielding 4.2 g of a clear, oily product. The oil contained (by GLC analysis) 15% **2** and the isomer pair **3** (1%) and **3a** (11%). Other products from this reaction were not characterized, although a number of products more volatile than the silicon rotanes, none in high yield, were observed. A similar condensation, but where the reaction solution was refluxed only an additional 0.3 h before quenching, led to 21% **2** and 12% **3**/**3a**. Analogous attempts using excess Na/K alloy also led to low yields of these cyclopolysilanes.

In one instance, a reaction in which the chlorosilane was added rapidly (3 min) to excess potassium was monitored by GLC. At 6 min following the addition, the solution contained 29% **2**, 1% **1**, and 7% **3**.[16a] The maximum yields of cyclosilanes (63%) occurred after 1.2 h, and the reaction solution then contained 57% **2**, 2% **1**, and 4% **3**. After 2.4 h, decreased yields were observed for **2** (43%) and **1** (1%), but the amount of **3**/**3a** increased slightly to 9%. Continued reflux led to decomposition, leaving only 2% **2** and 2% **3**/**3a** after 16.5 h.

Condensation of 2.0 equiv of potassium (3.9 g, 100 mmol) with $(CH_2)_4SiCl_2$ (7.8 g, 50 mmol) in 150 mL of dry, refluxing THF (1.3 h addition of chlorosilane, then 1.0 h additional reflux) formed 23% **2** and 14% **3**/**3a** as the only cyclosilanes present (GLC analysis). A reaction of $(CH_2)_4SiCl_2$ (50 mmol) with sodium (2.5 g, 110 mmol) and 150 mL of dry, refluxing toluene gave 13% **1**, 5% **2**, and 1% **3**/**3a** as the only cyclic compounds.

Synthesis of Cyclopentamethylene Silicon Rotanes. 1. Reaction of $(CH_2)_5SiCl_2$ with Potassium. Addition of $(CH_2)_5SiCl_2$ (3.4 g, 20 mmol) to excess potassium (1.7 g, 44 mmol) in 60 mL of dry THF followed by 18 h of reflux produced 1.83 g of a white solid. GLC analysis showed the solid to contain **5** (40%) and **6** (11%). Attempted separation by HPLC was unsuccessful due to the low solubility of these rotanes, and the cyclosilanes were instead purified by recrystallization. The crude product was partially dissolved in an EtOH/THF solution and filtered hot; upon cooling, **6**, in 94% purity, crystallized from the solution. After a small amount of solvent was stripped off, the mother liquor was again cooled, giving 0.45 g (23%) of colorless crystals of pure **5**. Recrystallization of the **6** fraction yielded 0.21 g (6%).

For **5**: mp 110–110.5 °C; IR 506 (s), 431 (w), 340 (m); UV [$\lambda(\epsilon)$] 282 (970), 269 (970), 209 sh (30 000). Exact mass calcd 490.2745; measured 490.2760, dev 3.1 ppm. Anal. Calcd for $C_{25}H_{50}Si_5$: C, 61.14; H, 10.26. Found: C, 61.02; H, 10.36.

For **6**: mp glistening at 232 °C; preshrinkage 250–252 and 260–264 °C; melts with dec at 272 °C; IR 506 (m), 487 (w), 365 (w, sh), 351 (m); UV [λ (ϵ)] 267 sh (1600), 244 (6400), 204 sh (44 000). Exact mass calcd 588.3294; measured 588.3291, dev 0.5 ppm. Anal. cacld for $C_{30}H_{60}Si_6$: C, 61.14; H, 10.26. Found: C, 60.99; H, 10.15.

The ^1H NMR spectra of both compounds consisted of indistinct multiplets at about 0.80–1.10, 1.30–1.60, and 1.60–1.90 ppm. The ratio of intensities was 2:1:2, respectively.

The mass spectra of both compounds are similar, and some selected *m*/*e* (relative intensity) with possible assignment are listed for **6**: 590 (9.5, M + 2), 589 (17.0, M + 1), 588 (27.5, M^+), 197 (11.4, $[(CH_2)_5]_2Si_2H$), 169 (3.5, $[(CH_2)_5](C_3H_5)Si_2H_2$), 141 (1.4, $[(CH_2)_5](CH_3)Si_2H_2$), 99 (7.0, $(CH_2)_5SiH$), 97 (16.0, $(C_5H_8)SiH$), 71 (34.5, C_5H_{11}), 69 (54.9, C_5H_9), 44 (100).

Reaction of excess potassium and $(CH_2)_5SiCl_2$ (50 mmol) in THF followed by only 1.0 h of reflux gave **5** (43%), **6** (7%), and also 18% of an insoluble product, thought to be poly(cyclopentamethylenesilylene) polymer. A similar condensation reaction was followed by withdrawing aliquots by syringe, quenching the samples with 2-propanol, and analyzing the products by GLC. The chlorosilane was added over 2.0 h; after a further 0.5 h the mixture contained 28% **5**, 4% **6**, and 6% of a new product **4**, along with some insoluble polymer. Following 9 h of reflux the mixture contained 57% **5**, 13% **6**, 1% **4**, and 5% of the oxide *cyclo*-$[(CH_2)_5Si]_8O$ (**8**). After 54 h the products were **5** (64%), **6** (16%), and **8** (7%). Compound **8** was purified by preparative GLC and identified by its mass spectrum: 507 (1.4, M + 1), 506 (8.2, M^+), 409 (47.9, $[(CH_2)_5]_4Si_4OH$), 341 (100, $[(CH_2)_5]_3Si_4OH_3$), 309 (53.5, $[(CH_2)_5]_2(C_5H_9)Si_3O$), 295 (11.1, $[(CH_2)_5]_3Si_3H$), 196 (33.7, $C_{10}H_{20}Si_2$), 99 (5.2, $(CH_2)_5SiH$), 97 (31.8, C_5H_8SiH), 71 (24.3, C_5H_{11}), 69 (49.2, C_5H_9), 57 (30.6, C_4H_9), 55 (42.3, C_4H_7).

A reaction using 3.7 g of Na/K (78% potassium by weight, 110 mmol), 50 mmol of $(CH_2)_5SiCl_2$, and 150 mL of dry THF was stirred at 25 °C for 9 days. Workup gave 50% insoluble polymer, 24% **5**, and 3% **6**. Low yields of cyclosilanes were also obtained when reacting only 2.0 equiv (3.9 g, 100 mmol) of potassium in 150 mL of THF with $(CH_2)_5SiCl_2$ (50 mmol). The remainder of the product appeared to be composed of soluble and insoluble polymeric materials.

2. Reaction of $(CH_2)_5SiCl_2$ with Lithium and Sodium. The reaction of $(CH_2)_5SiCl_2$ with Li wire (THF, 0 °C) was found to proceed poorly, probably because of deactivation of the Li by a coating of a white, polymeric material. Several modifications of the procedure, including the use of activated Li or addition of $Ph_3SiSiMe_3$, led to similarly poor results. Typical yields of cyclosilanes in such attempts were ca. 7% **5** and 1% **6**.

When a solution of Li powder (0.15 g, 22 mmol) and $(CH_2)_5SiCl_2$ (1.7 g, 10 mmol) in 30 mL of dry THF was agitated with an ultrasonic bath, a deep blue color was formed. After 35 h at 25 °C, the amount of Li powder was visibly less, and the reaction was worked up in the usual manner. The yields of cyclosilanes were found to be 49% **5**, 5% **6**, and 4% **8**.

A reaction of excess Na spheres (2.53 g, 110 mmol) and $(CH_2)_5SiCl_2$ (50 mmol) in 140 mL of dry toluene was attempted following the analogous procedure used to synthesize $(Et_2Si)_4$ from Et_2SiCl_2 and sodium.[4] Following 48 h of reflux, the products consisted of a toluene soluble fraction, containing 35% **5**, 10% **4**, and a trace of a new product, later shown to be *cyclo*-$[(CH_2)_5Si]_4O$ (**9**), and 9% insoluble polymer. Attempted isolation of **4** by Kugelrohr distillation (150 °C, 0.1 torr) of the reaction products led to apparent decomposition of this tetrasilane. Compound **4** is most readily isolated from photolysis mixtures, as is described subsequently.

Rearrangement of 2 and 3 Using Ph_3SiLi. These reactions were carried out in Schlenk tubes equipped with a magnetic stirrer and an argon inlet. In a typical reaction, 100 mg of **2** (0.20 mmol) was dissolved in 2 mL of dry, freshly distilled THF and was degassed by using several cycles of the freeze–pump–thaw method. Next, 2 mL of a Ph_3SiLi solution (~0.20 mmol, freshly prepared from $Ph_3SiSiPh_3$ and Li powder in degassed THF[32]) was added and the solution stirred at 25 °C. The

Table X. Summary of Crystal Data and Intensity Collection

parameter	$[(CH_2)_5Si]_5$ (**5**)	$[(CH_2)_4Si]_5$ (**1**)
crystal dimensions, mm	0.4 × 0.5 × 0.95	0.6 × 0.6 × 0.8
temp, °C	−90 ± 5	−85 ± 5
cell parameters		
a, Å	13.310 (2)	15.246 (2)
b, Å	14.762 (2)	9.133 (1)
c, Å	14.968 (2)	18.452 (3)
β, deg	103.39 (1)	107.59 (1)
space group	$P2_1/c$	$P2_1/c$
Z	4	4
density		
calcd, g/cm^3	1.14	1.14
meas, g/cm^3 [a]	1.10	1.04
radiation	graphite monochromated Mo Kα ($\bar{\lambda}$ = 0.71073 Å)	graphite monochromated Mo Kα ($\bar{\lambda}$ = 0.71073 Å)
absorption coeff μ, cm^{-1}	2.20	2.50
scan range		
deg below $2\theta K_{\alpha_1}$	1.0	0.7
deg above $2\theta K_{\alpha_2}$	1.0	0.7
scan rate, deg/min	2.4–24.0	2.0–24.0
scan type	θ–2θ	θ–2θ
2θ limits, deg	3.5–54.9	3.5–54.9
$(\sin\theta)/\lambda_{max}$, $Å^{-1}$	0.649	0.649
unique data		
theoretical	6540	5620
observed, $F_o > 3\sigma(F_o)$	5814	4969

[a] The measured densities were determined by flotation at room temperature.

(32) Gilman, H.; Lichtenwalter, G. D. *J. Am. Chem. Soc.* **1958**, *80*, 608.

Table XI. Fractional Coordinates for $[(CH_2)_5Si]_5$

atom	x	y	z	B_{iso}	atom	x	y	z	B_{iso}
Si(1)	0.642194 (23)	0.364286 (22)	0.321446 (22)	1.32	H(6A)	0.8467 (12)	0.1929 (11)	0.4037 (11)	3.0 (3)
Si(2)	0.725199 (23)	0.240693 (21)	0.268502 (21)	1.26	H(6B)	0.7427 (12)	0.1522 (11)	0.4021 (11)	3.2 (4)
Si(3)	0.855708 (23)	0.304834 (21)	0.204616 (22)	1.29	H(7A)	0.8574 (13)	0.0393 (12)	0.3793 (12)	3.8 (4)
Si(4)	0.795205 (23)	0.453808 (21)	0.171993 (22)	1.29	H(7B)	0.8768 (12)	0.0831 (11)	0.2938 (11)	3.2 (3)
Si(5)	0.747344 (23)	0.489665 (21)	0.310100 (21)	1.28	H(8A)	0.7559 (12)	−0.0366 (12)	0.2560 (11)	3.9 (4)
C(1)	0.61107 (10)	0.33591 (9)	0.43548 (8)	1.91	H(8B)	0.6787 (12)	0.0154 (12)	0.3021 (11)	3.2 (3)
C(2)	0.52110 (11)	0.26780 (9)	0.42167 (9)	2.21	H(9A)	0.7423 (12)	0.0812 (11)	0.1447 (11)	2.9 (3)
C(3)	0.42261 (10)	0.30315 (9)	0.35795 (10)	2.14	H(9B)	0.6364 (13)	0.0310 (12)	0.1339 (12)	3.9 (4)
C(4)	0.42978 (9)	0.31578 (9)	0.25837 (9)	1.98	H(10A)	0.5751 (11)	0.1502 (10)	0.2183 (10)	2.4 (3)
C(5)	0.50910 (9)	0.38735 (9)	0.24623 (9)	1.92	H(10A)	0.6087 (12)	0.1909 (11)	0.1317 (11)	3.2 (4)
C(6)	0.79152 (10)	0.16378 (9)	0.36524 (9)	1.99	H(11A)	0.9948 (12)	0.2426 (10)	0.3141 (10)	2.8 (3)
C(7)	0.82394 (10)	0.07431 (10)	0.32764 (11)	2.39	H(11B)	0.9795 (12)	0.3424 (11)	0.3449 (10)	2.6 (3)
C(8)	0.73424 (10)	0.02347 (9)	0.26662 (11)	2.52	H(12A)	1.1344 (10)	0.3331 (10)	0.2965 (10)	2.0 (3)
C(9)	0.68705 (11)	0.07190 (9)	0.17663 (10)	2.31	H(12B)	1.0609 (10)	0.3982 (10)	0.2333 (10)	2.2 (3)
C(10)	0.63382 (9)	0.16121 (9)	0.18990 (9)	1.84	H(13A)	1.0971 (11)	0.2167 (10)	0.1904 (10)	2.4 (3)
C(11)	0.98255 (9)	0.30411 (8)	0.29374 (8)	1.79	H(13B)	1.1474 (12)	0.3022 (11)	0.1515 (11)	3.2 (4)
C(12)	1.07144 (9)	0.33622 (9)	0.25198 (9)	2.09	H(14A)	0.9802 (11)	0.3489 (10)	0.0659 (10)	2.4 (3)
C(13)	1.08435 (10)	0.27954 (10)	0.17016 (10)	2.21	H(14B)	1.0117 (11)	0.2522 (10)	0.0353 (9)	2.2 (3)
C(14)	0.99263 (10)	0.28314 (10)	0.08683 (9)	2.10	H(15A)	0.8368 (11)	0.2465 (11)	0.0510 (10)	2.7 (3)
C(15)	0.89258 (9)	0.24343 (9)	0.10579 (8)	1.83	H(15B)	0.9030 (12)	0.1780 (11)	0.1218 (11)	3.0 (3)
C(16)	0.87992 (9)	0.54177 (9)	0.13359 (9)	1.94	H(16A)	0.9116 (11)	0.5154 (10)	0.0863 (10)	2.6 (3)
C(17)	0.81660 (11)	0.62599 (9)	0.09426 (10)	2.22	H(16B)	0.9378 (12)	0.5572 (11)	0.1852 (11)	3.2 (3)
C(18)	0.72478 (11)	0.60557 (10)	0.01461 (10)	2.41	H(17A)	0.7913 (12)	0.6571 (11)	0.1461 (11)	2.7 (3)
C(19)	0.64095 (10)	0.54774 (9)	0.04067 (9)	2.25	H(17B)	0.8633 (12)	0.6706 (11)	0.0717 (11)	3.0 (3)
C(20)	0.67771 (9)	0.45167 (8)	0.07219 (8)	1.78	H(18A)	0.6975 (13)	0.6611 (12)	−0.0137 (12)	3.7 (4)
C(21)	0.86124 (9)	0.50034 (9)	0.41246 (9)	1.86	H(18B)	0.7486 (11)	0.5708 (11)	−0.0328 (10)	2.8 (3)
C(22)	0.82553 (10)	0.53480 (10)	0.49726 (8)	2.10	H(19A)	0.5847 (12)	0.5417 (12)	−0.0122 (12)	3.9 (4)
C(23)	0.76613 (10)	0.62438 (9)	0.48184 (9)	2.12	H(19B)	0.6135 (11)	0.5771 (11)	0.0906 (11)	2.8 (3)
C(24)	0.66249 (10)	0.61884 (9)	0.41141 (9)	2.03	H(20A)	0.6228 (11)	0.4160 (11)	0.0864 (10)	2.8 (3)
C(25)	0.67410 (9)	0.59907 (8)	0.31367 (8)	1.75	H(20B)	0.6965 (11)	0.4198 (11)	0.0214 (10)	2.9 (3)
H(1A)	0.5900 (11)	0.3915 (11)	0.4633 (10)	2.5 (3)	H(21A)	0.8970 (11)	0.4438 (11)	0.4253 (10)	2.8 (3)
H(1B)	0.6701 (12)	0.3117 (11)	0.4744 (10)	2.9 (3)	H(21B)	0.9101 (12)	0.5421 (11)	0.3982 (11)	3.1 (3)
H(2A)	0.5097 (12)	0.2535 (11)	0.4811 (11)	3.0 (3)	H(22A)	0.7819 (11)	0.4923 (10)	0.5154 (10)	2.4 (3)
H(2B)	0.5394 (11)	0.2097 (10)	0.3962 (10)	2.3 (3)	H(22B)	0.8849 (11)	0.5418 (11)	0.5493 (10)	2.9 (3)
H(3A)	0.4049 (11)	0.3610 (10)	0.3842 (10)	2.5 (3)	H(23A)	0.8076 (12)	0.6715 (11)	0.4610 (11)	3.2 (3)
H(3B)	0.3691 (12)	0.2625 (11)	0.3600 (11)	2.8 (3)	H(23B)	0.7534 (12)	0.6428 (10)	0.5407 (10)	2.8 (3)
H(4A)	0.3661 (12)	0.3312 (11)	0.2241 (11)	3.0 (3)	H(24A)	0.6245 (12)	0.6781 (11)	0.4115 (11)	3.2 (3)
H(4B)	0.4429 (12)	0.2569 (11)	0.2329 (10)	3.1 (3)	H(24B)	0.6209 (10)	0.5724 (10)	0.4314 (9)	1.9 (3)
H(5A)	0.4886 (11)	0.4473 (11)	0.2671 (10)	2.8 (3)	H(25A)	0.6041 (11)	0.5969 (10)	0.2709 (10)	2.2 (3)
H(5B)	0.5078 (12)	0.3891 (11)	0.1830 (11)	2.9 (3)	H(25B)	0.7101 (11)	0.6461 (9)	0.2955 (10)	2.1 (3)

[a] The numbers given in parentheses are the estimated standard deviations of the least significant digits. [b] Isotropic equivalents are given for the atoms that were refined anisotropically.

progress of the rearrangement was followed by GLC. The solution contained 82% **2**, 6% **3**/**3a**, and 5% **1** after 12 h, and 45% **2**, 40% **3**/**3a**, and 3% **1** following 72 h of stirring. After quenching, the products were separated by HPLC. The **3a**:**3** ratio was determined by ^{13}C NMR and was found to be approximately 15:1. In a similar fashion, stirring **3** (75 mg, 0.13 mmol) in a THF solution of Ph_3SiLi (~0.15 mmol) produced a mixture of **2** (73%), **1** (10%), and **3**/**3a** (8%) after 1.5 h. An additional 30.5 h of stirring led to 33% **2**, 32% **3**/**3a**, and 5% **1**. ^{13}C NMR showed the ratio of **3a**:**3** to be 16:1.

The proportions of **1**–**3** (prior to the apparent onset of **3a**) varied somewhat, in different runs, from 80–91% for **2**, 4–11% for **3**, and 5–9% for **1**. The average of these attempts was 86% 2, 7% **3**, and 7% **1**. Decomposition was rather severe in these reactions, and the formation of volatile side products (possibly oxidation products) was shown by GLC.

Pyrolysis of 2 and 3. A small portion (~50 mg) of pure **2** was sealed in a small, evacuated glass tube and pyrolyzed at 220 °C for ca. 72 h in a tube furnace. GLC showed the products to be **3** (5%), **1** (15%), and recovered **2** (80%). Examination of the mixture by ^{13}C NMR showed a clean spectrum in which only resonances due to the three rotanes were present. A second pyrolysis of **2**, for 82 h at 320 °C, gave 12% **1** and 88% **2**, but no **3** was detected. Heating **3** (~20 mg) at 220 °C, also for 72 h, led to 2% **1**, 3% **2**, and 95% **3**. The ^{13}C NMR showed the correct resonances for **3**, but the signals for **1** and **2** were too weak to be observed. Analogous pyrolyses under argon at 230 °C caused conversion of **2** to a mixture of 5% **1**, 8% **3**, and 87% **2** after 36 h, and conversion of **3** to a mixture of 3% **1**, 7% **2**, and 90% **3** after 48 h. No products other than these silicon rotanes were detected by GLC.

Reaction of $(Me_2Si)_6$ under these conditions were also examined. Pyrolysis of $(Me_2Si)_6$ (230 °C, 6 days) in an evacuated sealed tube gave 1% $(Me_2Si)_5$ and 99% recovered cyclohexasilane. The thermal redistribution was enhanced only slightly at higher temperature, forming 2% $(Me_2Si)_5$ and 98% $(Me_2Si)_6$ after 72 h at 320 °C.

Photolysis. Photolyses were carried out under argon in quartz tubes at 30 °C using spectrograde cyclohexane or isooctane. A Rayonet reactor equipped with low-pressure mercury lamps (254 nm) was used. When 20 mg (0.04 mmol) of **5** was dissolved in 1.5 mL of isooctane, degassed by the freeze–pump–thaw method, and photolyzed, 50% **4** and 32% **5** were present after 1 h. Several minor products were observed by GLC, and a polymeric precipitate was formed as well. $[(CH_2)_5Si]_4$, **4**, was isolated by preparative GLC as a colorless oil. Its ^1H NMR spectrum and mass spectrum were closely similar to those of **5** and **6**. Exact mass calcd for **4** 392.2196; obsd 392.2204, dev 2.0 ppm; UV [λ (ϵ)] 311 (170), 270 sh (650), 229 sh (9200), 210 sh (22000).

In another experiment, photolysis of **5** (49 mg, 0.10 mmol) in 4.0 mL of degassed cyclohexane in the presence of Et_3SiH (120 mg, 1.0 mmol) gave the following products after 1.5 h, as estimated by GLC: **5** (9%), **4** (11%), **9** (5%), and trapping products, $Et_3Si(CH_2)_5SiH$ (**10**) and $Et_3Si(CH_2)_5Si(CH_2)_5SiH$ (**11**) (42.7 and 14.1 mg, respectively; this is 67% and 15%, based on 3 equiv of $(CH_2)_5Si$ lost from the starting amount of **5**). A number of volatile products, all in rather low yield, were also observed. The products were isolated by GLC and identified by their mass spectra. For **10**: colorless oil; selected m/e (relative intensity) 216 (4.0, M + 2), 215 (14.2, M + 1), 214 (59.1, M^+), 185 (18.6, M − C_2H_5), 157 (4.2, M − C_2H_5 − C_2H_4), 129 (10.9, $(CH_2)_5Si_2H_3$), 115 (100, Et_3Si), 99 (14.4, $(CH_2)_5SiH$), 87 (86.9, Et_2SiH), 71 (18.0, C_5H_{11}), 59 (65.6, $EtSiH_2$). Exact mass calcd 214.1566; obsd 214.1573, dev 3.3 ppm.

For **11**: a colorless oil; selected m/e (relative intensity) 313 (1.8, M + 1), 312 (7.6, M^+), 283 (1.8, M − C_2H_5), 213 (7.3, $(CH_2)_5SiSiEt_3$), 196 (100, $C_{10}H_{20}Si_2$), 115 (15.9, Et_3Si), 99 (10.2, $(CH_2)_5SiH$), 97 (18.8, $(C_4H_8)SiH$), 87 (23.9, Et_2SiH), 71 (8.3, C_5H_{11}). Exact mass calcd 312.2115; obsd 312.2126, dev 3.5 ppm.

For **9**: colorless solid; selected m/e (relative intensity) 409 (8.0, M + 1), 408 (23.6, M^+), 309 (11.4, $[(CH_2)_5]_2(C_5H_9)Si_3O$), 295 (23.4, $[(CH_2)_5]_3Si_3H$), 196 (100, $C_{10}H_{20}Si_2$), 99 (21.3, $(CH_2)_5SiH$), 97 (34.8, $(C_5H_8)SiH$), 71 (21.1, C_5H_{11}). Exact mass calcd 408.2145; obsd 408.2156, dev 2.7 ppm.

A similar photolysis using 55 mg (0.11 mmol) of **2** and 120 mg (1.0 mmol) of Et_3SiH in 4 mL of degassed cyclohexane produced 39% **1** and

Table XII. Fractional Coordinates for $[(CH_2)_4Si]_5$

atom	x	y	z	B_{iso}
Si(1)	0.33344 (3)	0.81815 (5)	0.086387 (24)	1.63
Si(2)	0.324787 (29)	0.81717 (5)	0.211011 (24)	1.58
Si(3)	0.180804 (29)	0.92168 (5)	0.199912 (24)	1.62
Si(4)	0.177098 (29)	1.11392 (5)	0.114811 (25)	1.69
Si(5)	0.251262 (29)	1.02669 (5)	0.028698 (24)	1.65
C(1)	0.45197 (12)	0.80261 (20)	0.07195 (11)	2.17
C(2)	0.45051 (13)	0.65236 (20)	0.03424 (11)	2.31
C(3)	0.35275 (13)	0.61835 (20)	−0.01545 (10)	2.30
C(4)	0.28659 (13)	0.64351 (20)	0.03186 (10)	2.23
C(5)	0.42175 (12)	0.92771 (20)	0.27773 (10)	2.22
C(6)	0.49467 (12)	0.81003 (21)	0.31092 (11)	2.46
C(7)	0.44607 (13)	0.67621 (10)	0.33118 (10)	2.35
C(8)	0.36176 (13)	0.63626 (19)	0.26345 (10)	2.23
C(9)	0.16287 (14)	0.97779 (27)	0.29377 (11)	2.81
C(10)	0.07520 (27)	0.8964 (4)	0.29415 (24)	4.52
C(11)	0.0536 (3)	0.7734 (7)	0.24221 (21)	5.91
C(12)	0.07792 (13)	0.79342 (22)	0.17202 (14)	2.83
C(13)	0.06297 (12)	1.21036 (21)	0.06961 (11)	2.38
C(14)	0.09130 (14)	0.37290 (22)	0.07396 (12)	2.66
C(15)	0.16083 (14)	1.40001 (21)	0.15108 (12)	2.71
C(16)	0.23786 (12)	1.28449 (20)	0.16597 (10)	2.24
C(17)	0.17365 (14)	0.99147 (23)	−0.07207 (10)	2.52
C(18)	0.19525 (17)	1.1186 (3)	−0.11971 (12)	3.49
C(19)	0.29657 (16)	1.1556 (3)	−0.08835 (11)	3.18
C(20)	0.32400 (13)	1.17118 (20)	−0.00128 (10)	2.18
H(1A)	0.5025 (17)	0.8129 (24)	0.1164 (13)	2.9 (5)
H(1B)	0.4581 (15)	0.8803 (24)	0.0354 (12)	2.5 (4)
H(2A)	0.4675 (15)	0.5717 (25)	0.0727 (13)	2.9 (4)
H(2B)	0.4988 (20)	0.638 (3)	0.0107 (17)	5.2 (6)
H(3A)	0.3490 (15)	0.5192 (25)	−0.0344 (12)	2.7 (4)
H(3B)	0.3339 (16)	0.6874 (24)	−0.0595 (13)	3.2 (5)
H(4A)	0.2891 (15)	0.5605 (26)	0.0674 (13)	3.2 (5)
H(4B)	0.2250 (18)	0.6471 (27)	0.0029 (14)	3.5 (5)
H(5A)	0.3987 (15)	0.9745 (24)	0.3151 (13)	2.8 (4)
H(5B)	0.4436 (17)	1.0095 (28)	0.2546 (14)	3.7 (5)
H(6A)	0.5437 (16)	0.8469 (25)	0.3540 (13)	3.0 (5)
H(6B)	0.5260 (16)	0.7833 (26)	0.2717 (13)	3.2 (5)
H(7A)	0.4274 (18)	0.7028 (28)	0.3770 (15)	4.1 (5)
H(7B)	0.4919 (17)	0.5929 (28)	0.3484 (14)	3.9 (5)
H(8A)	0.3770 (16)	0.5733 (26)	0.2283 (13)	3.1 (5)
H(8B)	0.3123 (18)	0.5871 (28)	0.2782 (14)	3.9 (5)
H(9A)	0.2170 (28)	0.938 (4)	0.3324 (23)	8.6 (10)
H(9B)	0.1568 (20)	1.080 (3)	0.2947 (16)	5.3 (7)
H(10A)	0.0616 (24)	0.895 (4)	0.3328 (21)	6.9 (9)
H(10B)	0.003 (4)	0.952 (6)	0.234 (3)	12.7 (15)
H(11A)	−0.0052 (25)	0.726 (4)	0.2367 (19)	6.9 (8)
H(11B)	0.122 (6)	0.706 (9)	0.285 (5)	23 (3)
H(12A)	0.0284 (23)	0.846 (3)	0.1348 (18)	5.9 (7)
H(12B)	0.0870 (25)	0.705 (4)	0.1431 (21)	7.6 (9)
H(13A)	0.0300 (17)	1.1722 (26)	0.0161 (14)	3.6 (5)
H(13B)	0.0244 (16)	1.1960 (24)	0.1001 (13)	3.1 (5)
H(14A)	0.0396 (19)	1.439 (3)	0.0629 (15)	4.3 (6)
H(14B)	0.1174 (19)	1.4004 (29)	0.0344 (16)	4.5 (6)
H(15A)	0.1230 (16)	1.3926 (25)	0.1906 (13)	3.2 (5)
H(15B)	0.1844 (16)	1.5047 (25)	0.1561 (13)	3.4 (5)
H(16A)	0.2654 (17)	1.2717 (26)	0.2153 (14)	3.3 (5)
H(16B)	0.2869 (17)	1.3143 (23)	0.1483 (13)	3.0 (5)
H(17A)	0.1098 (20)	0.986 (3)	−0.0781 (15)	4.4 (6)
H(17B)	0.1897 (21)	0.909 (3)	−0.0863 (17)	5.3 (7)
H(18A)	0.1609 (26)	1.217 (4)	−0.1025 (20)	7.4 (9)
H(18B)	0.1761 (21)	1.099 (3)	−0.1707 (19)	5.7 (7)
H(19A)	0.3112 (16)	1.240 (3)	−0.1146 (13)	3.9 (5)
H(19B)	0.3231 (20)	1.060 (3)	−0.1015 (16)	5.5 (7)
H(20A)	0.3838 (17)	1.1607 (24)	0.0201 (12)	2.8 (5)
H(20B)	0.3063 (15)	1.2662 (27)	0.0106 (12)	2.9 (4)

[a] The estimated standard deviations of the least significant digits are given in parentheses.

42% unreacted **2** after 0.25 h. Trapped adducts $Et_3Si(CH_2)_4SiH$ (**12**) and $Et_3Si(CH_2)_4Si(CH_2)_4SiH$ (**13**) were present in 76% and 15% yields, respectively, based on loss of one cyclotetramethylene silylene from **2**. After extended photolysis (1.3 h), there was present 3% **2**, 26% **1**, 5% *cyclo*-$[(CH_2)_4Si]_4O$ (**14**) and 2% *cyclo*-$[(CH_2)_4Si]_4O_2$ (**15**). The yields of **12** and **13**, as estimated by GLC, were 33 and 20 mg, respectively; these are 50% and 21% yields based on the formation of 3 eqiv (0.33 mmol) of $(CH_2)_4Si$. The oxides and the trapping products were obtained by preparative GLC and identified by their mass spectra.

Table XIII. Magnitude of the SiC_5 Torsional Angles in $[(CH_2)_5Si]_5$

atoms	torsional angle, deg
Si(1)-C(1)-C(2)-C(3)	59.4
C(1)-C(2)-C(3)-C(4)	66
C(2)-C(3)-C(4)-C(5)	63.6
C(3)-C(4)-C(5)-Si(1)	54.5
C(4)-C(5)-Si(1)-C(1)	45.3
C(5)-Si(1)-C(1)-C(2)	47.1
Si(2)-C(6)-C(7)-C(8)	57.0
C(6)-C(7)-C(8)-C(9)	66.7
C(7)-C(8)-C(9)-C(10)	66.1
C(8)-C(9)-C(10)-Si(2)	56.1
C(9)-C(10)-Si(2)-C(6)	44.5
C(10)-Si(2)-C(6)-C(7)	44.8
Si(2)-C(11)-C(12)-C(13)	57.8
C(11)-C(12)-C(13)-C(14)	63.8
C(12)-C(13)-C(14)-C(15)	63.8
C(13)-C(14)-C(15)-Si(3)	57.8
C(14)-C(15)-Si(3)-C(11)	48.7
C(15)-Si(3)-C(11)-C(12)	48.7
Si(4)-C(16)-C(17)-C(18)	56.6
C(16)-C(17)-C(18)-C(19)	65.2
C(17)-C(18)-C(19)-C(20)	64.5
C(18)-C(19)-C(20)-Si(4)	56.3
C(19)-C(20)-Si(4)-C(16)	45.6
C(20)-Si(4)-C(16)-C(17)	45.3
Si(5)-C(21)-C(22)-C(23)	55.7
C(21)-C(22)-C(23)-C(24)	65.1
C(22)-C(23)-C(24)-C(25)	65.8
C(23)-C(24)-C(25)-Si(5)	57.5
C(24)-C(25)-Si(5)-C(21)	46.3
C(25)-Si(5)-C(21)-C(22)	45.1

Table XIV. Interatomic C-H Distances (Å) for $[(CH_2)_4Si]_5$[a]

C(1)-H(1A)	0.945 (24)	C(11)-H(11A)	0.97 (4)
C(1)-H(1B)	1.003 (22)	C(11)-H(11B)	1.26 (9)
C(2)-H(2A)	1.001 (23)	C(12)-H(12A)	0.98 (3)
C(2)-H(2B)	0.97 (3)	C(12)-H(12B)	1.00 (4)
C(3)-H(3A)	0.966 (23)	C(13)-H(13A)	1.024 (24)
C(3)-H(3B)	0.999 (23)	C(13)-H(13B)	0.938 (24)
C(4)-H(4A)	0.995 (24)	C(14)-H(14A)	0.966 (27)
C(4)-H(4B)	0.931 (25)	C(14)-H(14B)	0.964 (28)
C(5)-H(5A)	0.963 (22)	C(15)-H(15A)	1.059 (23)
C(5)-H(5B)	0.968 (25)	C(15)-H(15B)	1.016 (23)
C(6)-H(6A)	0.972 (23)	C(16)-H(16A)	0.888 (24)
C(6)-H(6B)	1.011 (23)	C(16)-H(16B)	0.942 (24)
C(7)-H(7A)	1.000 (26)	C(17)-H(17A)	0.948 (29)
C(7)-H(7B)	1.017 (25)	C(17)-H(17B)	0.86 (3)
C(8)-H(8A)	0.946 (24)	C(18)-H(18A)	1.12 (4)
C(8)-H(8B)	0.984 (26)	C(18)-H(18B)	0.95 (3)
C(9)-H(9A)	0.98 (4)	C(19)-H(19A)	0.973 (26)
C(9)-H(9B)	0.94 (3)	C(19)-H(19B)	1.03 (3)
C(10)-H(10A)	0.80 (4)	C(20)-H(20A)	0.883 (24)
C(10)-H(10B)	1.40 (6)	C(20)-H(20B)	0.954 (24)

[a] Average distance is 0.99 (10) Å.

For **13**: colorless oil; selected *m/e* (relative intensity) 200 (13.8, M^+), 115 (100, Et_3Si), 87 (68.0, Et_2SiH), 59 (23.5, $EtSiH_2$), 55 (6.0, C_4H_7). Exact mass calcd 200.1410; obsd 200.1416, dev 3.0 ppm.

For **13**: colorless oil; selected *m/e* (relative intensity) 285 (1.0 M + 1), 284 (7.5, M^+), 255 (1.0, M − C_2H_5), 168 (100, $C_8H_{16}Si_2$), 115 (25.7, Et_3Si), 87 (31.6, Et_2SiH), 83 (11.8, C_4H_6SiH), 59 (21.6, $EtSiH_2$), 55 (3.2, C_4H_7).

For **14**: colorless oil; selected *m/e* (relative intensity) 354 (14.0, M + 2), 353 (27.1, M + U), 352 (91.3, M^+), 311 (13.4, M − C_3H_5), 269 (20.8, $[(CH_2)_4]_3Si_3OH$), 268 (26.8), 267 (100, $[(CH_2)_4]_2(C_4H_7)SiO_3$?), 185 (14.4, $[(CH_2)_4]_2Si_2OH$), 168 (18.9, $C_8H_{16}Si_2$), 85 (37.0, $(CH_2)_4SiH$), 83 (53.8, C_4H_6SiH), 57 (42.8, C_4H_9), 55 (19.3, C_4H_7).

For **15**: colorless oil; selected *m/e* (relative intensity) 369 (4.5, M + 1), 368 (19.0, M^+), 339 (0.2, M − C_2H_5), 283 (4.5, $[(CH_2)_4]_2(C_4H_7)$-Si_3O_2), 168 (100, $C_8H_{16}Si_2$), 85 (18.1, $(CH_2)_4SiH$), 83 (27.1, (C_4H_6)-SiH), 57 (16.6, C_4H_9).

A product, believed to be $[(CH_2)_4Si]_4$ based on its retention time, was also detected by using GLC from this photolysis. The maximum yield

Table XV. Interatomic C–H Distances (Å) for $[(CH_2)_5Si]_5$[a]

C(1)–H(1A)	0.990 (16)	C(13)–H(13B)	1.001 (16)
C(1)–H(1B)	0.934 (16)	C(14)–H(14A)	1.022 (15)
C(2)–H(2A)	0.960 (16)	C(14)–H(14B)	0.980 (14)
C(2)–H(2B)	0.992 (15)	C(15)–H(15A)	0.972 (15)
C(3)–H(3A)	0.991 (15)	C(15)–H(15B)	0.997 (17)
C(3)–H(3B)	0.937 (16)	C(16)–H(16A)	0.984 (15)
C(4)–H(4A)	0.912 (16)	C(16)–H(16B)	0.983 (16)
C(4)–H(4B)	0.981 (16)	C(17)–H(17A)	1.024 (16)
C(5)–H(5A)	0.998 (16)	C(17)–H(17B)	1.016 (16)
C(5)–H(5B)	0.943 (16)	C(18)–H(18A)	0.955 (18)
C(6)–H(6A)	0.927 (16)	C(18)–H(18B)	0.986 (16)
C(6)–H(6B)	0.961 (17)	C(19)–H(19A)	0.960 (17)
C(7)–H(7A)	0.950 (18)	C(19)–H(19B)	1.004 (16)
C(7)–H(7B)	0.967 (16)	C(20)–H(20A)	0.963 (16)
C(8)–H(8A)	0.957 (16)	C(20)–H(20B)	0.975 (16)
C(8)–H(8B)	1.013 (16)	C(21)–H(21A)	0.958 (16)
C(9)–H(9A)	0.975 (16)	C(21)–H(21B)	0.956 (16)
C(9)–H(9B)	1.014 (18)	C(22)–H(22A)	0.937 (15)
C(10)–H(10A)	0.986 (15)	C(22)–H(22B)	0.978 (15)
C(10)–H(10B)	0.963 (16)	C(23)–H(23A)	0.983 (17)
C(11)–H(11A)	0.960 (16)	C(23)–H(23B)	0.974 (16)
C(11)–H(11B)	0.961 (16)	C(24)–H(24A)	1.011 (17)
C(12)–H(12A)	0.943 (14)	C(24)–H(24B)	0.971 (14)
C(12)–H(12B)	0.958 (15)	C(25)–H(25A)	1.001 (14)
C(13)–H(13A)	0.979 (16)	C(25)–H(25B)	0.919 (15)

[a] Average distance is 0.97 (3) Å.

(7%) was present after 0.8 h of photolysis. Attempted isolation by preparative GLC gave samples whose mass spectra were identical with that of **15**. No other products were observed in significant yield.

Crystal Structures of 1 and 5. X-ray Data Collection. Single crystals of both compounds were grown by vapor diffusion of MeOH into a THF solution. Both studies were carried out on a Syntex-Nicolet P_1 four-circle diffractometer equipped with a modified LT-1 low-temperature device. Unit cell parameters were obtained from least-squares refinements based on the setting angles of 60 reflections collected at $\pm 2\theta$ ($|2\theta| \sim 35°$) at the same temperature as the data collection. The dimensions of the crystals, the unit cell parameters, and other crystal data are given in Table X. Delauney cell reductions did not reveal any hidden symmetry.

Intensity data were collected with the crystals used for the preliminary examinations. Details of the intensity measurements are given in Table X. Four standard reflections from diverse regions of reciprocal space were measured every 50 reflections throughout data collection to monitor the long term stability. There were no significant trends for either compound. Structure amplitudes and their standard deviations were calculated from the intensity data by procedures similar to those described previously.[33] Absorption correctons were not applied.

Structure Solution and Refinement. The structures were solved by direct methods using the MULTAN package.[34] The positions of the silicon atoms were revealed by the E maps, and the carbon atoms were located by subsequent electron density difference maps. The full-matrix least-squares refinements of the structures were based on F_o and used the reflections with $F_o > 3\sigma(F_o)$. Both structures were initially refined to convergence using isotropic thermal parameters for the non-hydrogen atoms. Electron density difference maps revealed the positions for all the hydrogen atoms. In the final cycles of refinement all non-hydrogen atoms were assumed to vibrate anisotropically and all hydrogen atoms were assumed to vibrate isotropically. The parameters for the hydrogen atoms were included with those varied in the final cycles. Atomic form factors were taken from Cromer and Waber[35] and that for hydrogen was taken from Stewart et al.[36]

The final values of the discrepancy indices for **5** were $R_1 = \sum||F_o| - |F_c||/\sum|F_o| = 0.029$ and $R_2 = [\sum w(|F_o| - |F_c|)^2/\sum w(F_o)^2]^{1/2} = 0.040$. The estimated standard deviation of an observation of unit weight was 1.49, with a final data/variable ratio of 12.3. The final electron density difference map was featureless. Final atomic coordinates are given in Table XI and selected distances and angles are given in Tables IV and V.

The final values of the discrepancy indices for **1** were $R_1 = 0.035$ and $R_2 = 0.057$. The estimated standard deviation of an observation of unit weight was 2.05 with a data/variable ratio of 12.9. There were no significant features on the final electron density difference map. Final atomic coordinates are given in Table XII and selected distances and angles are given in Tables II and III.

Listings of the SiC_5 torsional angles in $[(CH_2)_5Si]_5$ and the C–H distances for both $[(CH_2)_4Si]_5$ and $[(CH_2)_5Si]_5$ are given in Tables XIII–XV.

Acknowledgment. This work was supported by the U.S. Air Force Office of Scientific Research, Air Force System Command, USAF, under Grant AFOSR 82-0067. The United States Government is authorized to reproduce and distribute reprints for governmental purposes notwithstanding any copyright notation thereon.

Registry No. 1, 84081-92-5; **2**, 84098-37-3; **3**, 84098-38-4; **3a**, 84081-96-9; **4**, 91178-60-8; **5**, 84081-94-7; **6**, 84081-95-8; **8**, 91178-61-9; **9**, 91178-62-0; **10**, 91178-63-1; **11**, 91178-64-2; **12**, 91178-65-3; **13**, 91178-66-4; **14**, 91178-67-5; $[(CH_2)_4Si]_8$, 84081-93-6; $[(CH_2)_4Si]_9$, 84098-39-5; $[(CH_2)_4Si]_{10}$, 89098-40-8; $[(CH_2)_4Si]_{11}$, 84098-41-9; $[(CH_2)_4Si]_{12}$, 84098-42-0; $(CH_2)_4SiCl_2$, 2406-33-9; $(CH_2)_5SiCl_2$, 2406-34-0; $(Me_2Si)_6$, 4098-30-0; $(Me_2Si)_5$, 13452-92-1; Li, 7439-93-2; K, 7440-09-7; poly(cyclopentamethylenesilylene), 91178-68-6.

Supplementary Material Available: Listings of fractional atomic coordinates, anisotropic thermal parameters, and structure factors for compounds **1** and **5** (54 pages). Ordering information is given on any current masthead page.

(33) Haller, K. J.; Enemark, J. H. *Inorg. Chem.* **1978**, *17*, 3552.
(34) Germain, G.; Main, P.; Woolfson, M. M. *Acta Crystallogr., Sect. A* **1971**, *A27*, 368.
(35) Cromer, D. T.; Waber, J. T. "Internaltional Tables for X-ray Crystallography"; Kynoch Press: Birmingham, England, 1974; Vol. 4, pp 99–101, Table 2.2B.
(36) Stewart, R. F.; Davidson, E. R.; Simpson, W. T. *J. Chem. Phys.* **1965**, *42*, 3175.